WIND-TUNNEL INVESTIGATION OF AERODYNAMIC CHARACTERISTICS OF A 1/2-SCALE MODEL OF AN EJECTION SEAT WITH A RIGID-WING RECOVERY SYSTEM

by Sanger M. Burk, Jr.

Langley Research Center
Hampton, Va. 23365

NATIONAL AERONAUTICS AND SPACE ADMINISTRATION • WASHINGTON, D. C. • AUGUST 1970

1. Report No.	2. Government Accession No.	3. Recipient's Catalog No.
NASA TN D-5922		

4. Title and Subtitle

WIND-TUNNEL INVESTIGATION OF AERODYNAMIC CHARACTERISTICS OF A 1/2-SCALE MODEL OF AN EJECTION SEAT WITH A RIGID-WING RECOVERY SYSTEM

5. Report Date: August 1970

6. Performing Organization Code:

7. Author(s)

Sanger M. Burk, Jr.

8. Performing Organization Report No.: L-7185

9. Performing Organization Name and Address

NASA Langley Research Center
Hampton, Va. 23365

10. Work Unit No.: 124-07-19-03

11. Contract or Grant No.:

12. Sponsoring Agency Name and Address

National Aeronautics and Space Administration
Washington, D.C. 20546

13. Type of Report and Period Covered: Technical Note

14. Sponsoring Agency Code:

15. Supplementary Notes

16. Abstract

A wind-tunnel investigation has been conducted in the Langley full-scale tunnel to determine the static longitudinal and lateral characteristics of a model of an ejection seat equipped with a rigid-wing recovery system. Several wing and vertical-tail arrangements were tested as well as various configurations of the ejection seat alone, ranging from unfaired to completely faired seats.

17. Key Words (Suggested by Author(s))

Emergency escape systems
Low-speed aerodynamics
Static stability and control
Ejection seat

18. Distribution Statement

Unclassified – Unlimited

19. Security Classif. (of this report)	20. Security Classif. (of this page)	21. No. of Pages	22. Price*
Unclassified	Unclassified	37	$3.00

*For sale by the Clearinghouse for Federal Scientific and Technical Information
Springfield, Virginia 22151

WIND-TUNNEL INVESTIGATION OF AERODYNAMIC CHARACTERISTICS OF A 1/2-SCALE MODEL OF AN EJECTION SEAT WITH A RIGID-WING RECOVERY SYSTEM

By Sanger M. Burk, Jr.
Langley Research Center

SUMMARY

A wind-tunnel investigation has been made at low subsonic speeds to determine the static longitudinal and lateral aerodynamic characteristics of a model of an ejection seat equipped with a rigid-wing recovery system. The investigation was intended to provide some preliminary information for determining the feasibility of such a concept with primary emphasis on static stability and control.

The results of the investigation indicated that the concept was feasible from static stability and control considerations. All the configurations were statically longitudinally stable until the stall. The lateral stability characteristics were more configuration dependent; the high-wing—high-tail arrangements showed better effective dihedral characteristics but had reduced directional stability. The low-wing—low-tail arrangements gave better directional stability characteristics but had negative effective dihedral. Although representative full-scale performance measurements were not possible in the low-scale tests, it appeared that the performance of the configurations was high enough to warrant further consideration of the concept for recovery purposes. The performance, as expected, was highly dependent upon the relative sizes of the wing and fuselage combinations.

INTRODUCTION

The U.S. Air Force and U.S. Navy are interested in developing new concepts for rescuing aircrew members who are forced to abandon their aircraft over unfavorable territory. The ultimate goal is to provide aircrews with an escape system having a powered-flight capability and thus enable the crew to fly toward more favorable territory.

The Langley Research Center has investigated various types of recovery systems for aircraft, spacecraft, and boosters. Some typical results are reported in references 1 to 5. As a continuing part of this research program, an investigation has been made to determine the performance and static stability and control characteristics of a rigid-wing

aircrew recovery system attached to an encapsulated ejection seat. A propulsion system was not simulated in this investigation. Effects of wing size and position were investigated as well as vertical-tail size and position. The aerodynamic characteristics of the wing-alone configurations and of various ejection-seat-alone configurations, ranging from unfaired to completely faired seats, were determined in order to ascertain the relative benefits of streamlining. Longitudinal aerodynamic characteristics of the complete model were obtained at 0° sideslip through an angle-of-attack range. The lateral stability characteristics for the complete-model configurations were obtained over approximately the same angle-of-attack range at sideslip angles of $\pm 10^{\circ}$. A few tests were made to determine the control effectiveness of the all-movable vertical tails.

SYMBOLS

The longitudinal and lateral data are referred to the wind and body axis systems, respectively, as shown in figure 1. The origin of the axes is located at the center-of-gravity position shown in figure 2. Longitudinally, the position is located at 25 percent of the mean aerodynamic chord of each wing. Units used for the physical quantities in this paper are given in the U.S. Customary Units and in the International System of Units (SI). Factors relating the two systems are given in reference 6.

b wing span, ft (m)

C_D drag coefficient of wing-alone or complete-model configurations, D/qS

$C_{D,s}$ drag coefficient of ejection-seat-alone configurations, D/qS_s

C_L lift coefficient of wing-alone or complete-model configurations, L/qS

$C_{L,s}$ lift coefficient of ejection-seat-alone configurations, L/qS_s

C_l rolling-moment coefficient of complete-model configurations, $\frac{\text{Rolling moment}}{qSb}$

$C_{l_\beta} = \frac{\partial C_l}{\partial \beta}$, per deg

C_m pitching-moment coefficient of wing-alone or complete-model configurations, $\frac{\text{Pitching moment}}{qSc}$

$C_{m,s}$ pitching-moment coefficient of ejection-seat-alone configurations, $\frac{\text{Pitching moment}}{qS_sH}$

C_n yawing-moment coefficient of complete-model configurations, $\frac{\text{Yawing moment}}{qSb}$

$C_{n_\beta} = \frac{\partial C_n}{\partial \beta}$, per deg

C_Y lateral-force coefficient of complete-model configurations, $\frac{\text{Lateral force}}{qS}$

$C_{Y_\beta} = \frac{\partial C_Y}{\partial \beta}$, per deg

c wing chord, ft (m)

D drag, lb (N)

H height of back of ejection seat, 1.70 ft (0.518 m)

L lift, lb (N)

L/D lift-drag ratio

q free-stream dynamic pressure, lb/ft^2 (N/m^2)

R Reynolds number

S wing area, ft^2 (m^2)

S_S area of back of ejection seat, 1.37 ft^2 (0.127 m^2)

X,Y,Z body axes

α angle of attack of wing-alone or complete-model configurations (reference line is wing chord plane), deg

α_s angle of attack of ejection seat (reference line is bottom of seat), deg (see fig. 1)

β angle of sideslip of complete-model configurations, deg

δ_h deflection of all-movable horizontal tail (positive with trailing edge down), deg

DESIGN CONSIDERATIONS

Although the rigid-wing recovery system was not designed specifically to meet the Air Force and Navy requirements for an advanced self-rescue system, these requirements did influence the design approach. The services desire a self-propelled system capable of a range of 50 miles (80 km) at a speed of 100 knots (51.4 m/sec). It is not necessary that the system be capable of landing since the crewman will descend on his personnel parachute at an appropriate time.

For simplicity, a conventional wing concept was selected. Factors considered in sizing the small wing were: (1) it would be used only for cruising flight, (2) it would not exceed the height of the ejection seat when folded against the sides, and (3) the chord would be large enough to provide reasonable wing loading without unduly restricting the pilot's visibility when folded. The large wing selected for comparison purposes would have to telescope or have an additional folding section. In order to facilitate stowage, fairly thin airfoil sections were selected, and it was assumed that the vertical and horizontal tails would be made of flexible material and attached to a telescoping boom. It might be desirable to rigidify these surfaces after deployment by ram- or compressed-air inflation or by the use of quick-solidifying foam plastic injected between the surfaces.

From a human factors standpoint, an erect position for the man and seat was believed to be best and for reasonable flight performance, the seat should be streamlined. The winged ejection seat would be flown by a fly-by-wire system incorporating stability augmentation and utilizing a two-control system – all-movable vertical and horizontal tails. A possible deployment sequence for a configuration is shown in figure 3. The front fairing is indicated as being telescoping, and the aft fairing presumably would be inflatable.

MODELS AND APPARATUS

Models

The models used in the investigation were of rigid construction and were considered to be approximately 1/2-scale. Three complete-model configurations were used, and three-view drawings of these models are presented in figure 2. Pertinent dimensions of

the complete models are given in tables I and figure 2. All the configurations utilized the ejection seat equipped with a telescoping front fairing and an aft fairing. Six different versions of the ejection seat were provided as shown in the sketches of figure 4. Photographs of two of the seat configurations are shown in figure 5. Two unswept rectangular wings with NACA 0009 air foil sections were used; one wing had twice the area and approximately 50 percent greater aspect ratio than the other one. (See table I.) Hereinafter, these two wings will be referred to as small and large wings.

The all-movable vertical- and horizontal-tail surfaces were constructed of balsa and had triangular planforms, flat cross sections, rounded leading edges, and beveled trailing edges. The vertical tails consisted of upper and lower surfaces which were identical in size and which were used singly or in combination. These configurations and their locations are shown in figure 6.

Test Equipment

The static force tests were conducted in the Langley full-scale tunnel, a detailed description of which is given in reference 7. The tests were made by using sting-type support equipment and a six-component strain-gage balance. Because of the various locations of the wings and vertical-tail surfaces, different model mounting methods had to be used. Photographs of the models and the mounting methods used in the tunnel are shown in figure 7.

TESTS

Force tests were made to determine the static longitudinal aerodynamic characteristics of the various ejection-seat-alone configurations over a range of angles of attack generally from 0° to 52° at zero sideslip. The aerodynamic characteristics of the wing-alone configurations and the complete-model configurations were obtained over an angle-of-attack range from -1° to 32°. The static lateral aerodynamic characteristics of the complete-model configurations were determined from tests made at various angles of attack over a sideslip range of $\pm 10^{\circ}$. Tests also were made to determine the effect of configuration changes, such as wing size and location, and vertical-tail size and location. Additional tests were conducted to determine the control effectiveness of the vertical- and horizontal-tail surfaces.

All tests were conducted at a dynamic pressure of 2.68 lb/ft^2 (128.3 N/m^2). The test Reynolds number based on the chord of the small wing (1.083 ft (0.330 m)) was 330 000 and based on the chord of the large wing (1.250 ft (0.381 m)) was 380 000.

RESULTS AND DISCUSSION

Longitudinal Stability and Control Characteristics

Ejection seat alone.- The longitudinal aerodynamic characteristics of the ejection-seat-alone configurations are shown in figure 8. The data indicate, as might be expected, that the seat with the greatest streamlining (configuration 6), that is, both fore and aft fairings attached to the seat, had the least drag, whereas the seat (configuration 1) with no fairings had the greatest drag. However, the drag of the seats equipped with front fairings increased with an increase in angle of attack primarily because the flat seat bottoms of these configurations resulted in increased frontal area as the angle of attack increased. The drag of the seats without front fairings decreased with increasing angle of attack because the projected frontal area of the seats was decreased.

These data also show that there were wide variations in the lift characteristics of the various configurations and that all the configurations were longitudinally unstable as indicated by the variation of the pitching-moment curve with angle of attack.

Wings alone.- The longitudinal aerodynamic characteristics of the configurations with small and large wings alone are shown in figure 9. Also included in this figure are full-scale Reynolds number lift and drag data obtained from estimates and from tests reported in reference 8. A comparison of these data show that the scale effects for the particular wings investigated were very large in terms of maximum lift-drag ratios, maximum lift, and stall angle of attack. Therefore, the small-scale data cannot be used directly for realistic performance predictions, and caution should be used in applying the results in analysis studies at full scale. The lift and drag data are included in the present paper for use in interpreting the longitudinal and lateral stability characteristics and for use in relative performance comparisons between the different configurations investigated.

Complete models.- The effect of horizontal-tail deflection on the longitudinal aerodynamic characteristics of the complete-model configurations is presented in figure 10. A comparison of the untrimmed longitudinal characteristics of the configuration is presented in figure 11, and the trimmed lift-drag ratios are presented in figure 12. The data in figure 10 show that all the configurations are longitudinally stable until the stall but that although the horizontal tail is capable of trimming the configurations from zero to maximum lift, there are substantial differences in the control characteristics between configurations. The data of figure 12 indicate that configuration I (small wing in low position) and configuration II (small wing in high position) had maximum trimmed L/D values of 3.7 and 3.6, respectively. Configuration III (large wing in high position) with the higher aspect ratio (6.3) had a maximum trimmed L/D of 6.0. It should be noted that on the basis of the differences in the low- and high-scale wing-alone data of figure 9, the values of L/D for the complete-model configuration would probably be somewhat higher

at full-scale Reynolds number than those indicated in the present report. Also, the fact that the lift coefficient corresponding to the maximum value of L/D occurred close to the stall in the model tests is not considered significant in terms of full-scale conditions because the stall angle of attack and lift coefficient at full scale would be much higher than those shown in model tests and the necessary usable lift margins for flight safety could be easily achieved. Thus, although representative full-scale performance measurements were not possible in the low-scale tests, it appears that the performance of the configurations is sufficient to warrant further consideration of the concept for recovery purposes.

Lateral Stability and Control Characteristics

The variation of the lateral coefficients C_Y, C_n, and C_l with angle of sideslip for various angles of attack and vertical-tail sizes for configurations I, II, and III is presented in figures 13, 14, and 15, respectively. These data are summarized in figure 16 in the form of the stability derivatives C_{Y_β}, C_{n_β}, and C_{l_β} plotted against angle of attack. The values of the derivatives were obtained by taking the difference between the values of the coefficients measured at sideslip angles of $\pm 5^\circ$. Since some of the data are nonlinear, these derivatives should be used only to indicate trends and to provide approximate comparisons of various configurations.

Lateral stability characteristics.- In developing the configurations, it was desired that the models be directionally stable and have positive effective dihedral $\left(-C_{l_\beta}\right)$ at least up to the stall. The data of figure 16(a) show that configuration I is directionally stable with several vertical-tail arrangements but the model had negative effective dihedral for these tail arrangements almost until the stall. The negative effective dihedral of configuration I was not unexpected since the wing had 0° geometric dihedral and was in a low position relative to the capsule. It appears that the incorporation of some geometric dihedral might provide positive effective dihedral in the angle-of-attack range for maximum L/D ($\alpha \approx 10^\circ$).

Both configurations II and III had positive effective dihedral over the angle-of-attack range for all tail arrangements. The top and bottom vertical-tail arrangement provided the greatest amount of directional stability at low angles of attack, but the directional stability decreased as the angle of attack increased so that the directional stability was marginal or neutral in the 10° to 15° angle-of-attack range. These data show that larger vertical tails are required to provide the desired level of directional stability for the high-wing configurations. This result is to be expected because of the characteristic effect of wing height on sidewash at the tail.

It is evident from the data of figure 16 that the lateral characteristics of the fly-away ejection seat are greatly dependent upon the geometry of the configuration. The

contributions of the vertical tails are influenced by whether or not they are in the wake of the capsule and the effective dihedral is particularly influenced by the wing-capsule arrangement although the effective dihedral was also sometimes greatly influenced by the tail configuration.

Lateral-directional control characteristics.- The variation with angle of attack of the incremental control-moment coefficients produced by deflecting the all-movable vertical tail $\pm 10^{o}$ is shown in figure 17 for configuration I (only control-moment data measured). Data are presented for the configurations with both the top and bottom vertical tails and the bottom tail alone. The results indicate that deflecting the all-movable vertical tails for both configurations produced favorable yawing and rolling moments that were almost constant over the angle-of-attack range. Deflecting both the top and bottom vertical tails produced approximately twice the force and moments of the bottom vertical tail.

Although it is realized that the force and moments provided by these surfaces would not produce the desired roll and sideslip responses on a configuration with negative effective dihedral, these control characteristics are considered representative of what this type of control surface would produce.

SUMMARY OF RESULTS

The results of an investigation to determine the aerodynamic characteristics of a model of an ejection seat with a rigid-wing recovery system indicated that the concept was feasible from static stability and control considerations. All the configurations were statically longitudinally stable until the stall. The lateral stability characteristics were more configuration dependent; the high-wing—high-tail arrangements showed better effective dihedral characteristics but had reduced directional stability. The low-wing—low-tail arrangements gave better directional stability characteristics but had negative effective dihedral. Although representative full-scale performance measurements were not possible in the low-scale tests, it appeared that the performance of the configurations was sufficient to warrant further consideration of the concept for recovery purposes. The performance, as expected, was highly dependent upon the relative sizes of the wing and fuselage combinations.

Langley Research Center,
National Aeronautics and Space Administration,
Hampton, Va., June 29, 1970.

REFERENCES

1. Scher, Stanley H.; and Draper, John W.: The Effects of Stability of Spin-Recovery Tail Parachutes on the Behavior of Airplanes in Gliding Flight and in Spins. NACA TN 2098, 1950.

2. Burk, Sanger M., Jr.; and Healy, Frederick M.: Comparison of Model and Full-Scale Spin Recoveries Obtained by Use of Rockets. NACA TN 3068, 1954.

3. Lee, Henry A.; and Burk, Sanger M., Jr.: Low-Speed Dynamic-Model Investigation of Apollo Command Module Configurations in the Langley Spin Tunnel. NASA TN D-3888, 1967.

4. Bugg, Frank M.; and Sleeman, William C., Jr.: Low-Speed Tests of an All-Flexible Parawing for Landing a Lifting-Body Spacecraft. NASA TN D-4010, 1967.

5. Burk, Sanger M., Jr.: Free-Flight Investigation of the Deployment, Dynamic Stability, and Control Characteristics of a 1/12-Scale Dynamic Radio-Controlled Model of a Large Booster and Parawing. NASA TN D-1932, 1963.

6. Mechtly, E. A.: The International System of Units – Physical Constants and Conversion Factors. NASA SP-7012, 1964.

7. DeFrance, Smith J.: The NACA Full-Scale Wind Tunnel. NACA Rep. 459, 1933.

8. Goett, Harry J.; and Bullivant, W. Kenneth: Tests of NACA 0009, 0012, and 0018 Airfoils in the Full-Scale Tunnel. NACA Rep. 647, 1938.

TABLE I.- GEOMETRIC CHARACTERISTICS OF WINGS AND TAIL SURFACES

Small wing:	
Span, ft (m)	4.55 (1.39)
Area, ft^2 (m^2)	4.93 (0.46)
Chord, ft (m)	1.083 (0.330)
Aspect ratio	4.2
Airfoil section	NACA 0009
Large wing:	
Span, ft (m)	7.88 (2.40)
Area, ft^2 (m^2)	9.85 (0.92)
Chord, ft (m)	1.250 (0.381)
Aspect ratio	6.3
Airfoil section	NACA 0009
Horizontal tail (including boom):	
Span, ft (m)	1.60 (0.49)
Area, ft^2 (m^2)	0.73 (0.068)
Aspect ratio	3.5
Airfoil section	Flat plate
Vertical tails:	
Top and bottom tails (including boom):	
Height, ft (m)	2.18 (0.66)
Area, ft^2 (m^2)	1.37 (0.13)
Aspect ratio	3.47
Airfoil section	Flat plate
Top or bottom tail:	
Height exposed, ft (m)	1.01 (0.31)
Area exposed, ft^2 (m^2)	0.59 (0.055)
Aspect ratio	1.73
Airfoil section	Flat plate

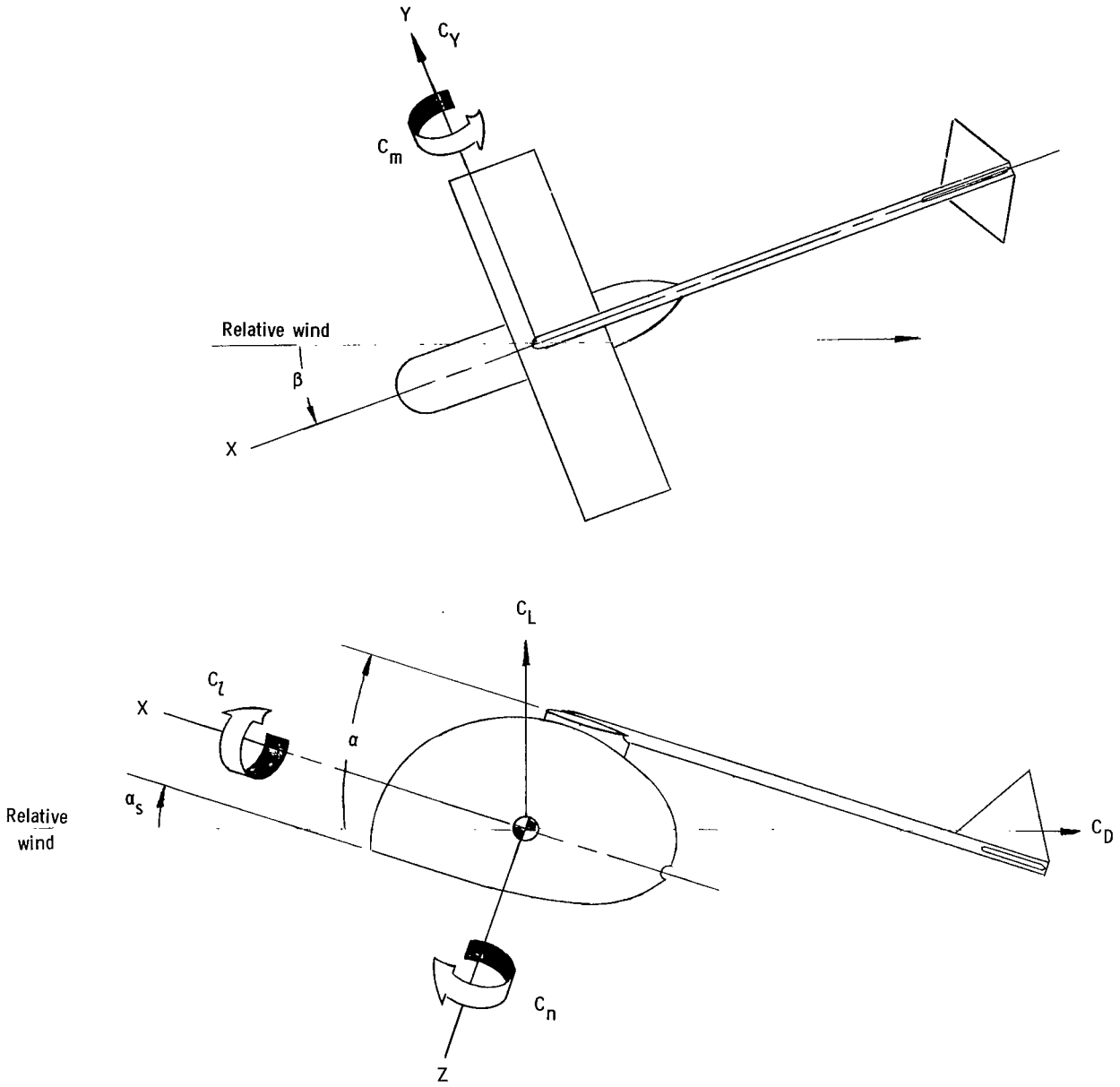

Figure 1.- Axis systems used in investigation. Longitudinal and lateral data are referred to wind and body axes, respectively. Arrows indicate positive directions of moments, forces, and angles.

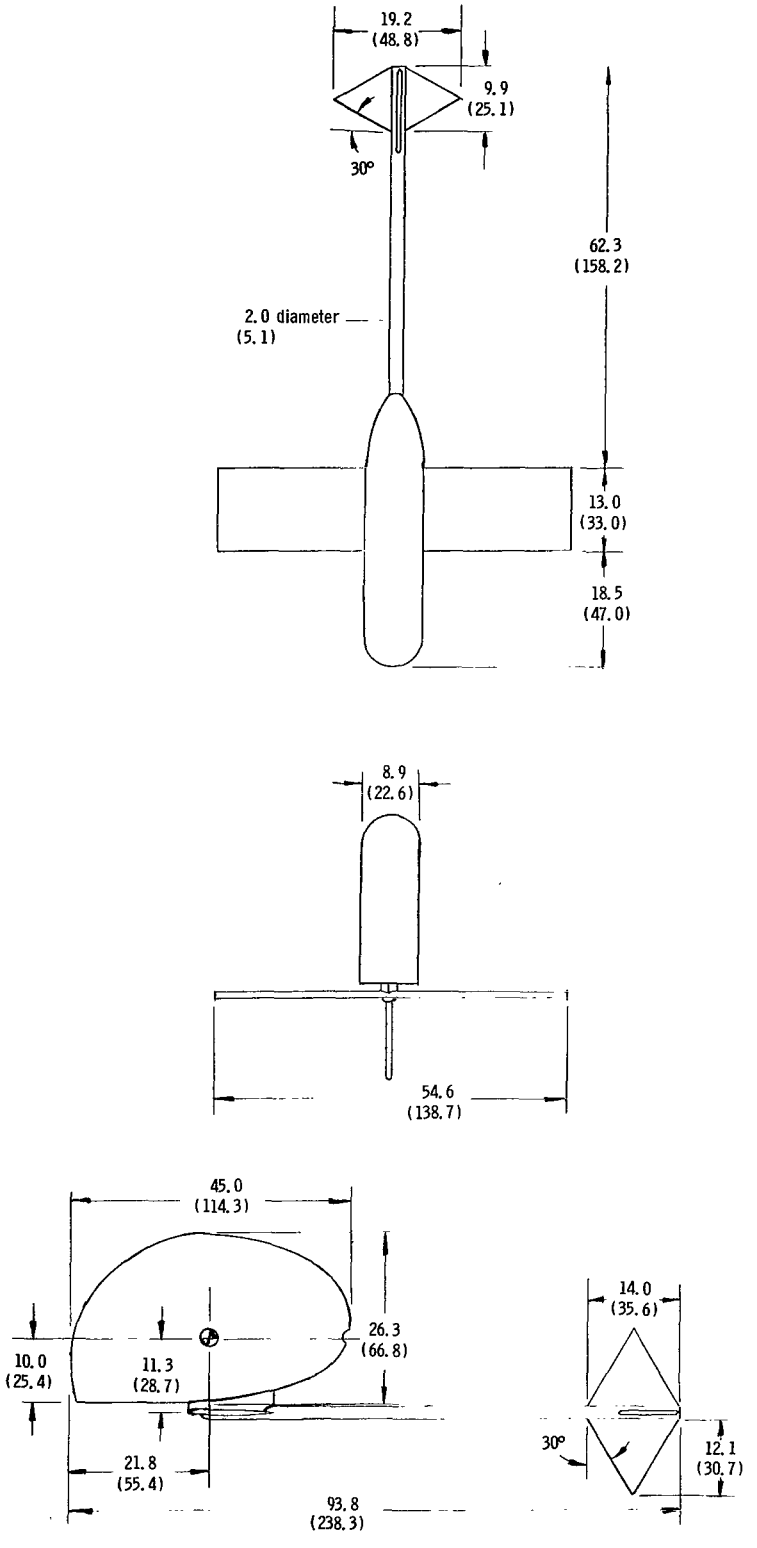

(a) Configuration I (small wing in low position).

Figure 2.- Three-view drawing of complete-model configuration. Dimensions are in inches (centimeters).

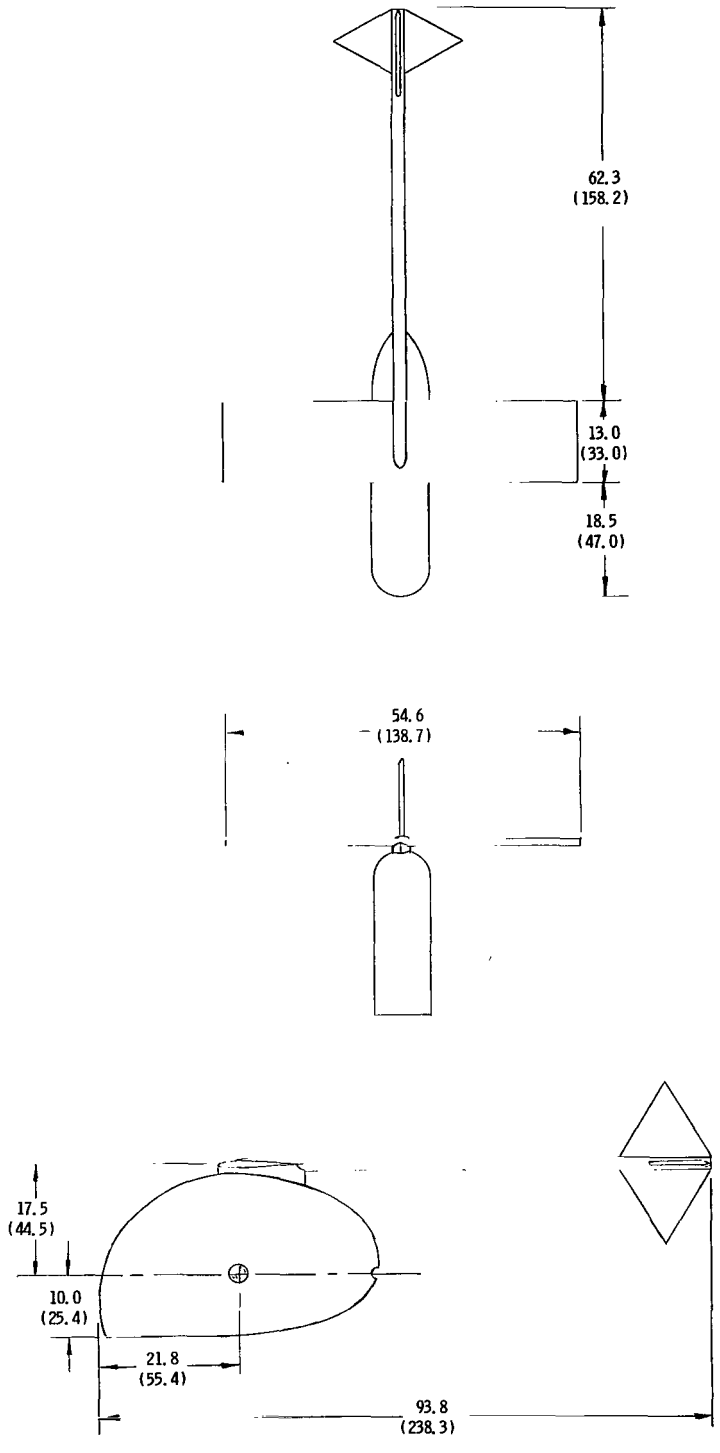

(b) Configuration II (small wing in high position).

Figure 2.- Continued.

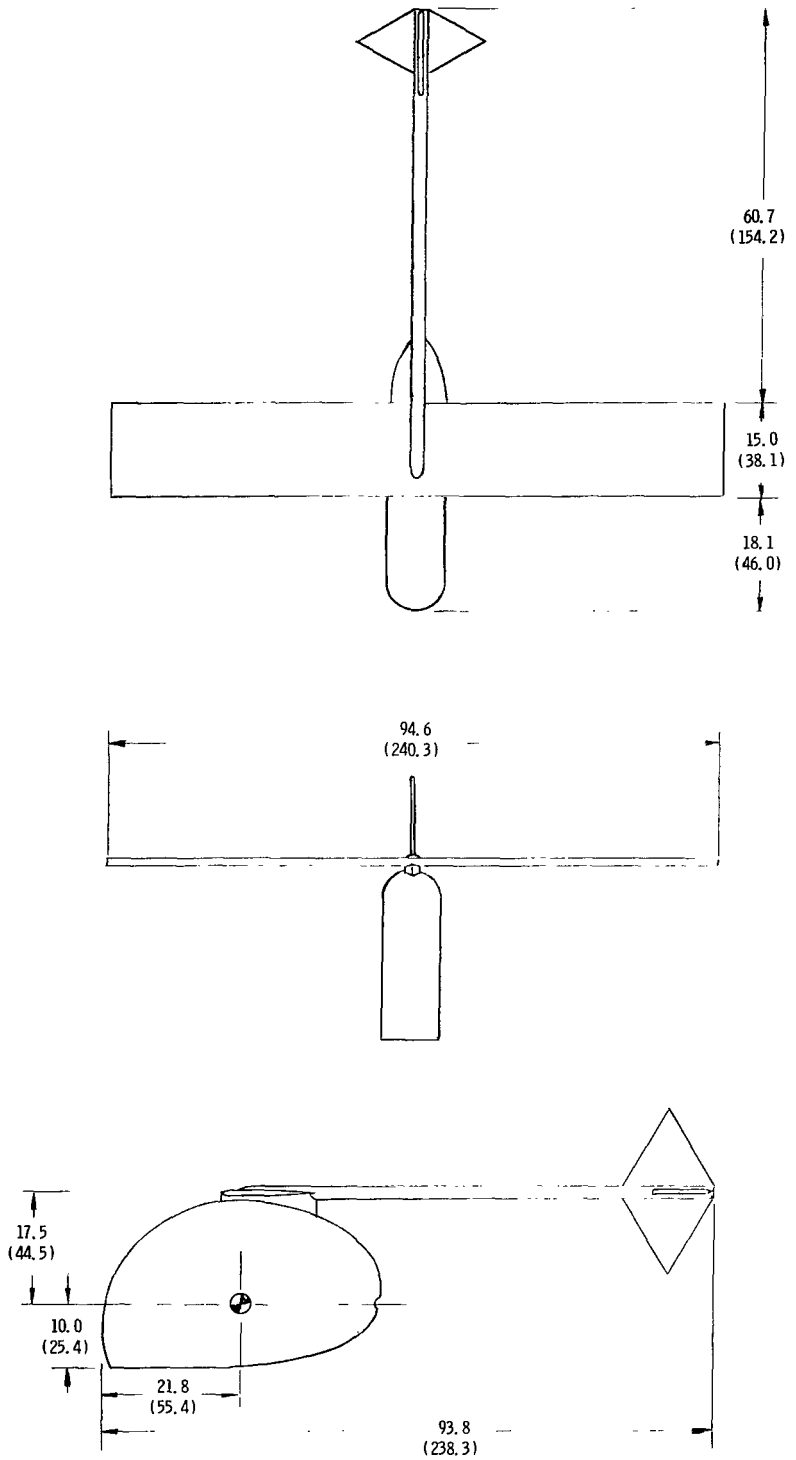

(c) Configuration III (large wing in high position).

Figure 2.- Concluded.

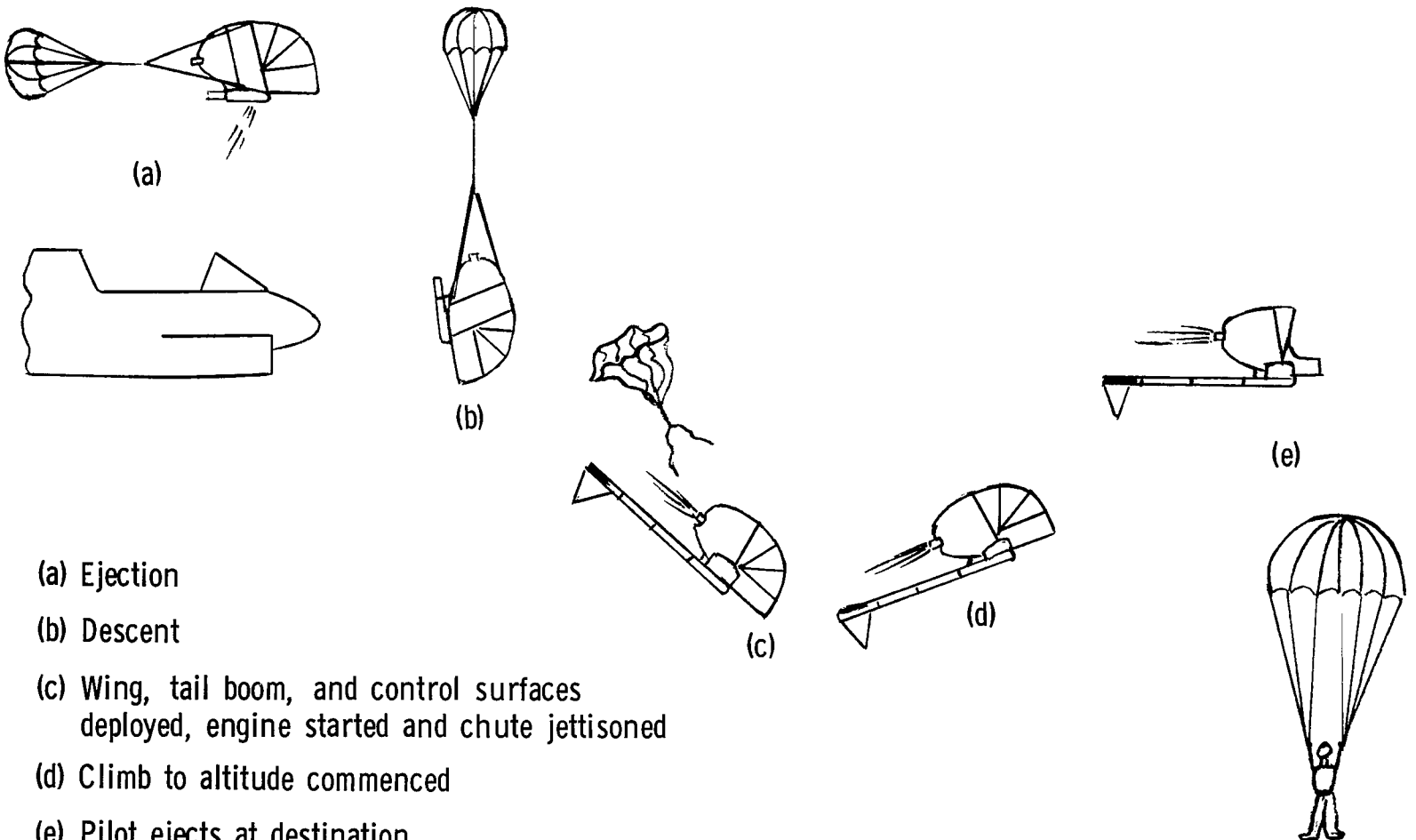

Figure 3.- Possible deployment sequence.

(1) Unoccupied seat.

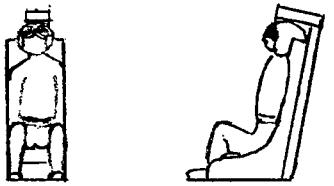

(2) Dummy pilot in seat.

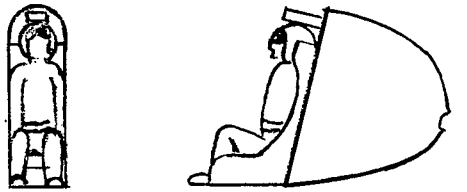

(3) Dummy pilot plus aft fairing.

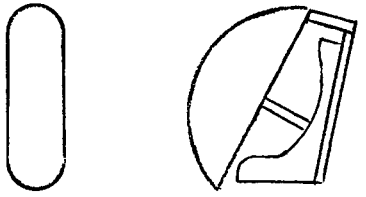

(4) Unbrella-type front fairing.

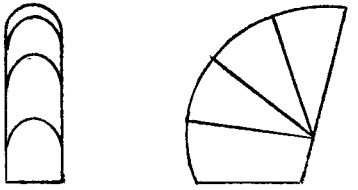

(5) Telescoping front fairing.

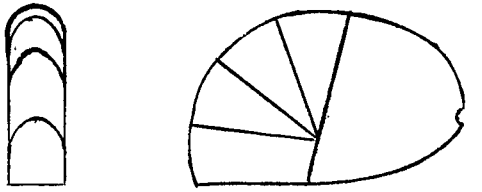

(6) Telescoping front fairing plus aft fairing.

Figure 4.- Ejection-seat-alone configurations.

(a) Configuration 2 (dummy pilot in seat).

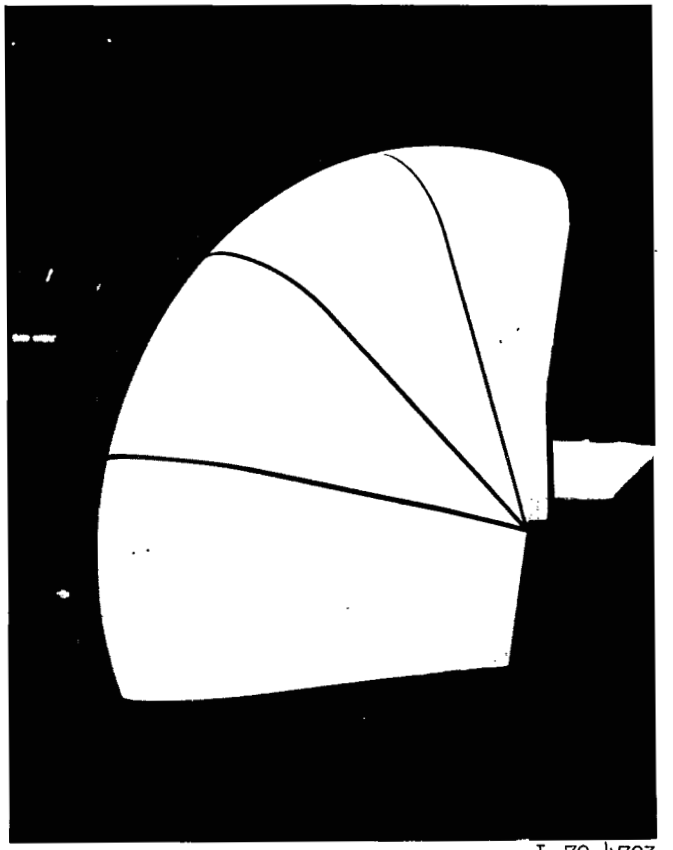

L-70-4703

(b) Configuration 5 (telescoping front fairing).

Figure 5.- Two ejection-seat-alone configurations.

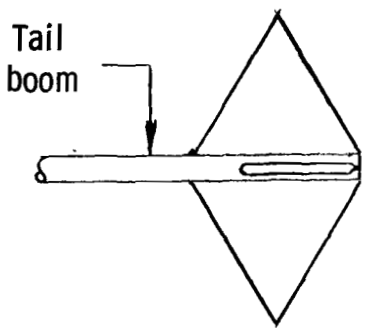

(a) Top and bottom vertical tails.

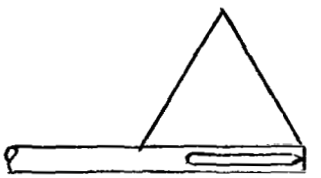

(b) Top vertical tail.

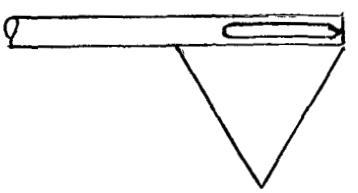

(c) Bottom vertical tail.

Figure 6.- Vertical-tail configurations.

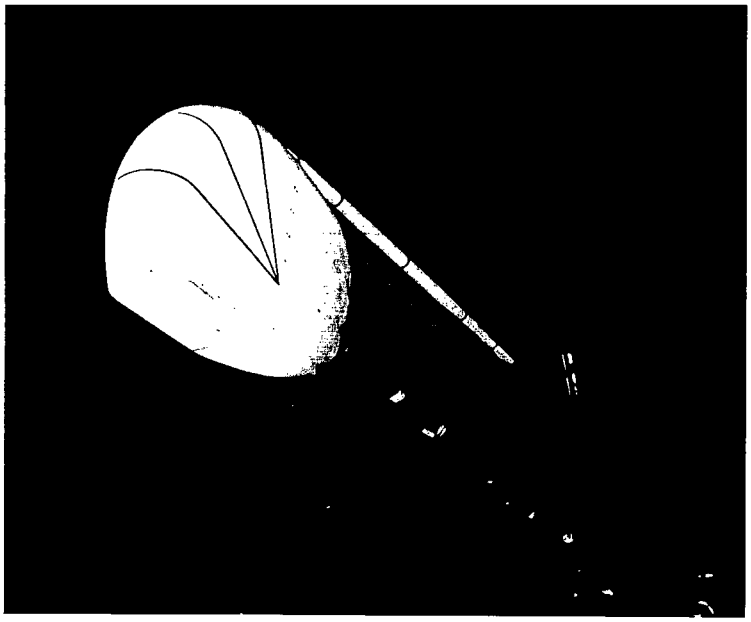

(a) Straight sting. L-69-4388

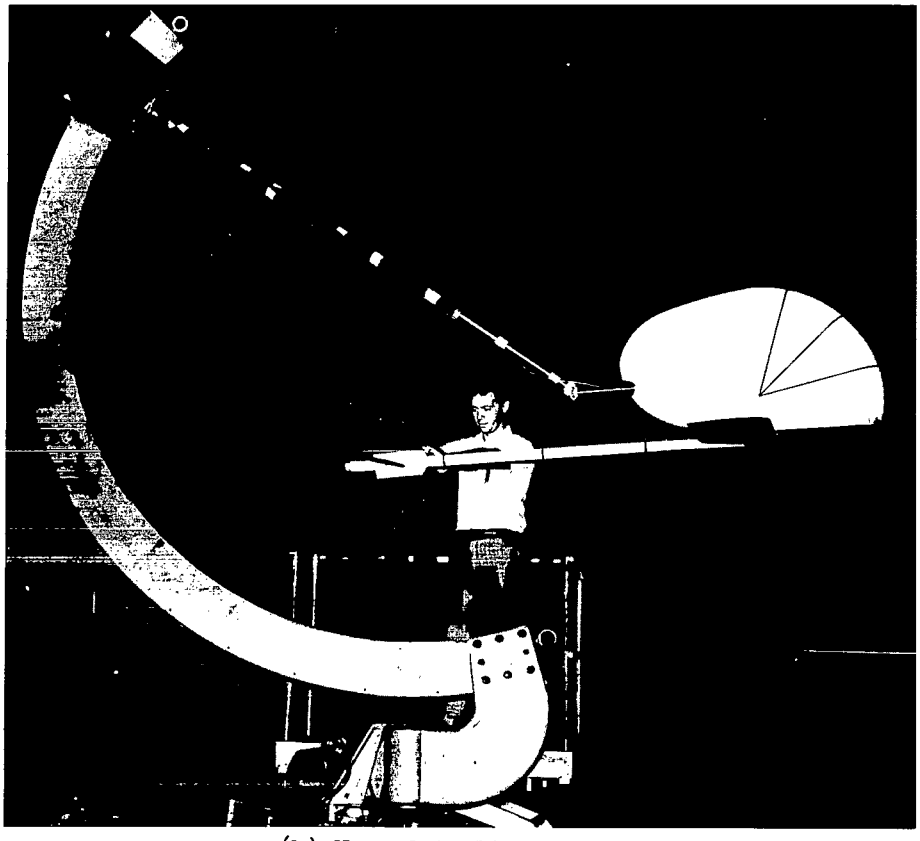

(b) Upward inclined sting. L-69-7420

Figure 7.- Model mounting methods in Langley full-scale tunnel.

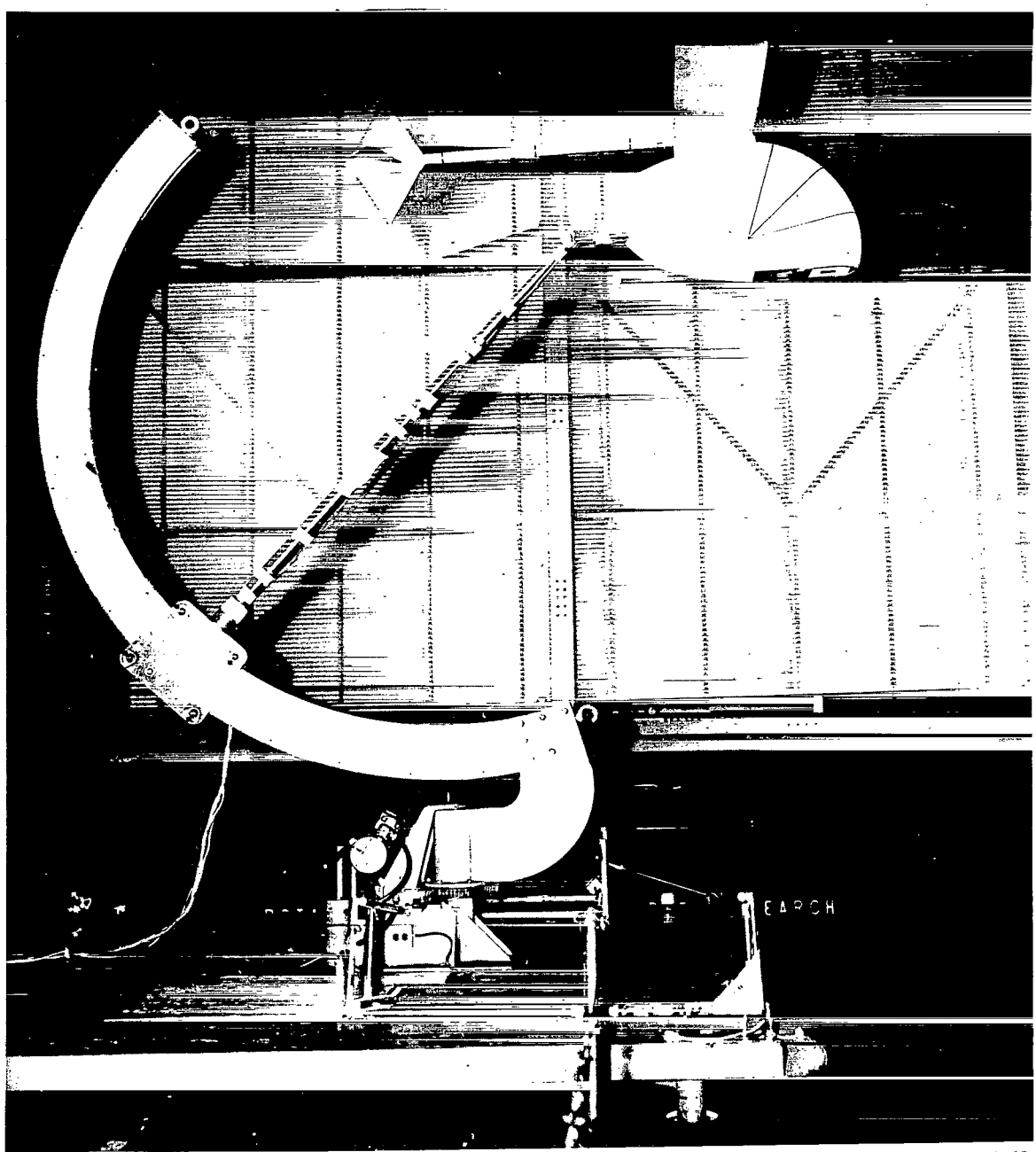

(c) Downward inclined sting. L-69-7468

Figure 7.- Concluded.

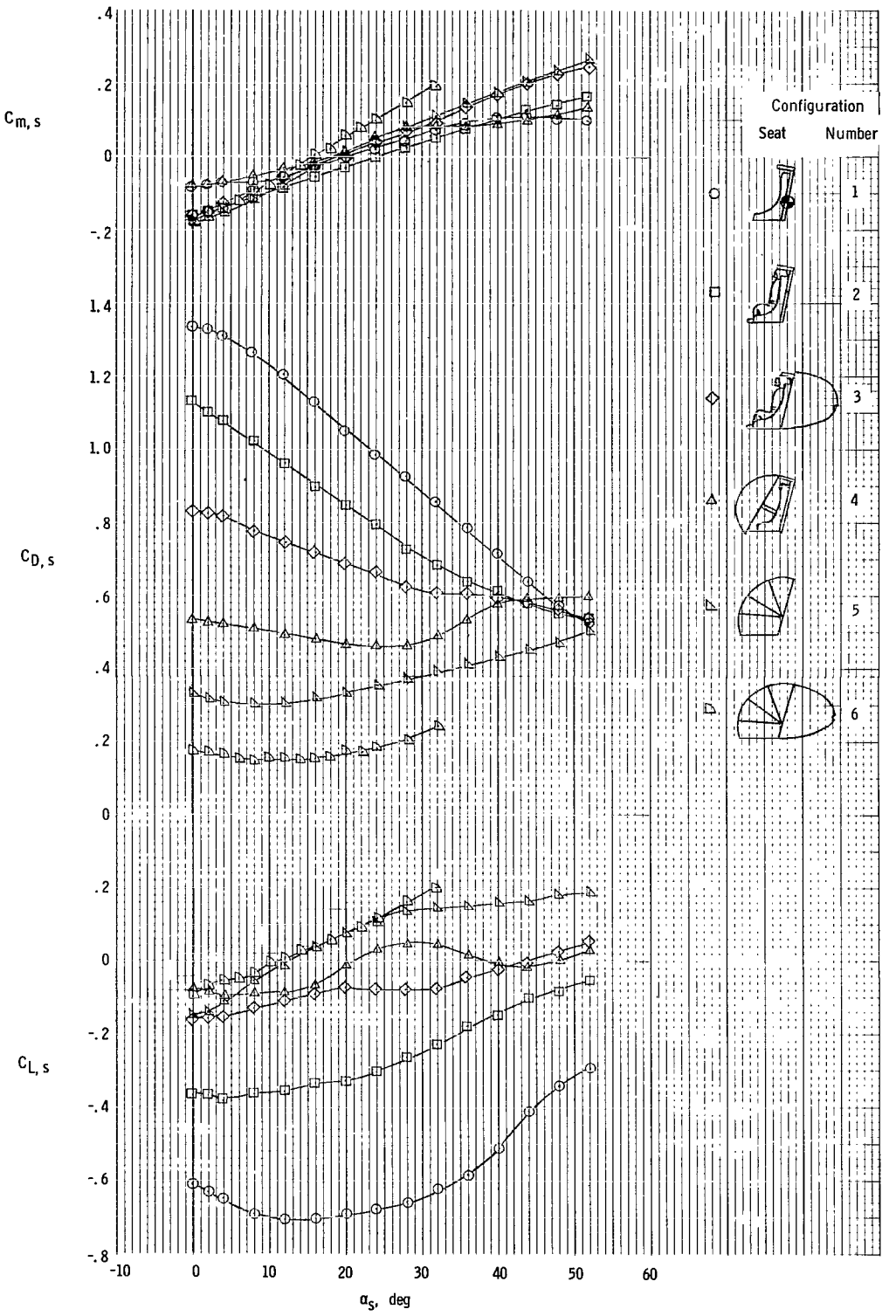

Figure 8.- Longitudinal aerodynamic characteristics of ejection-seat-alone configurations.

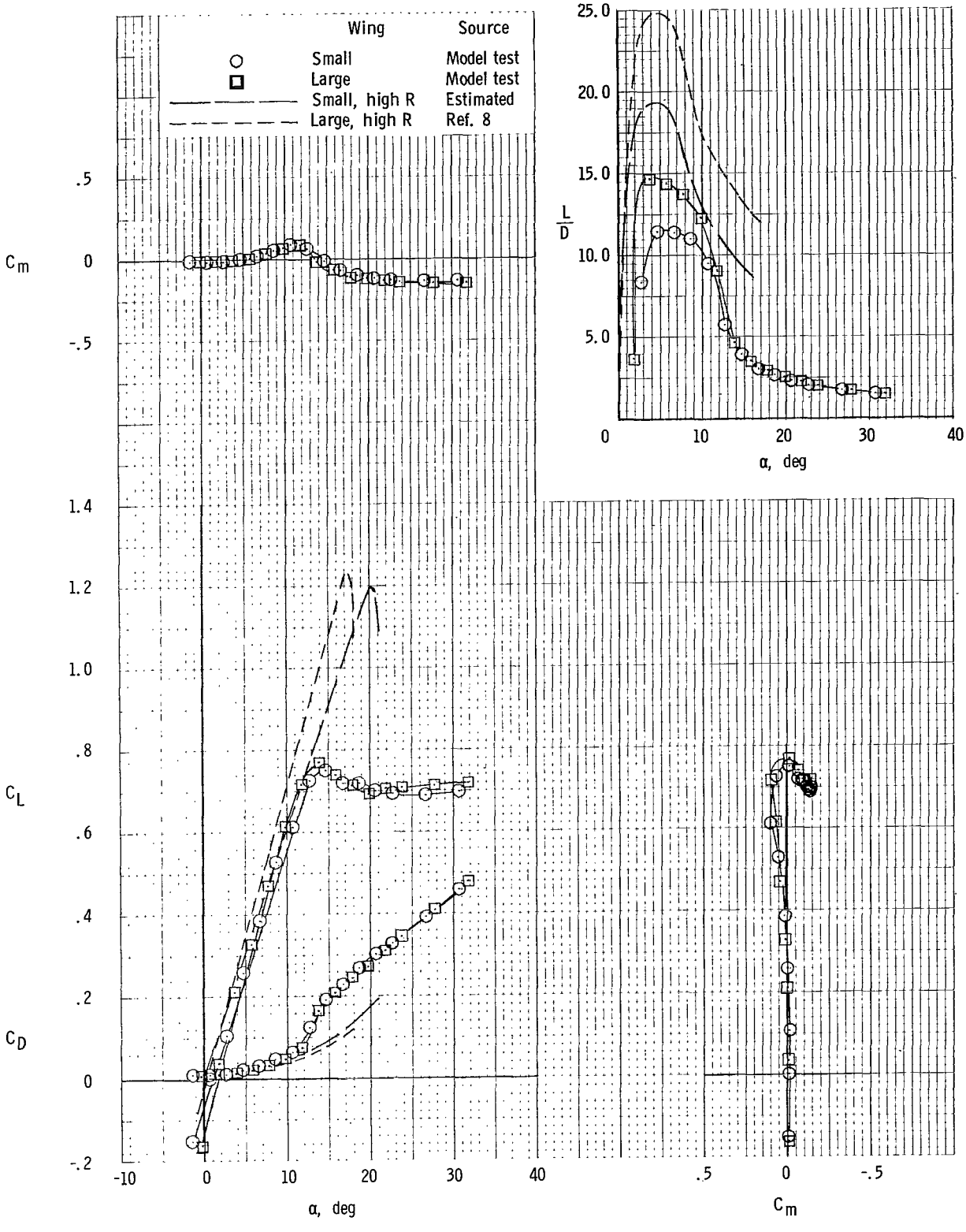

Figure 9.- Comparison of longitudinal aerodynamic characteristics of configurations with small and large wings alone.

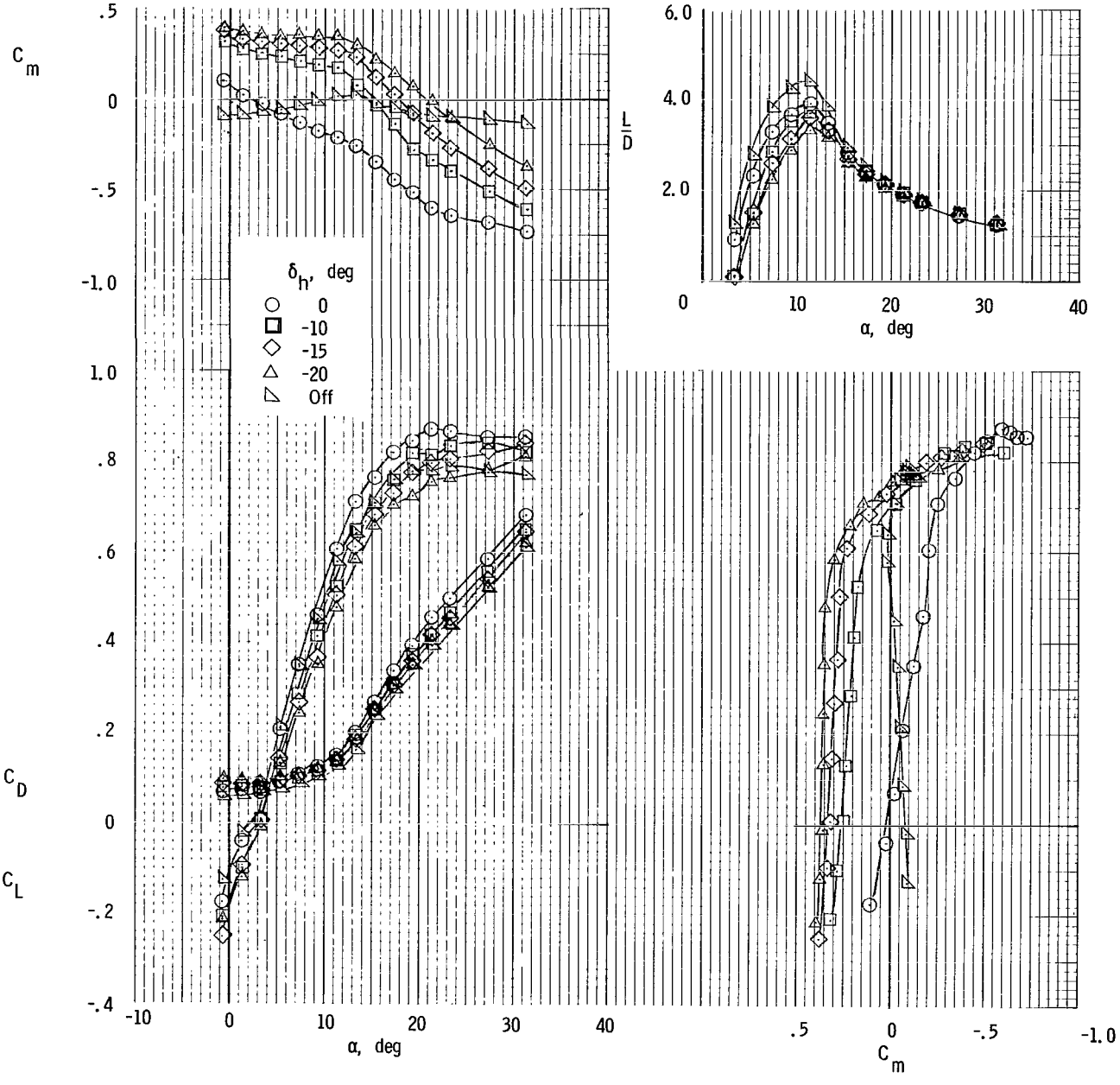

(a) Configuration I (small wing in low position).

Figure 10.- Effect of horizontal-tail deflections on longitudinal aerodynamic characteristics of complete-model configurations. Top vertical tail on.

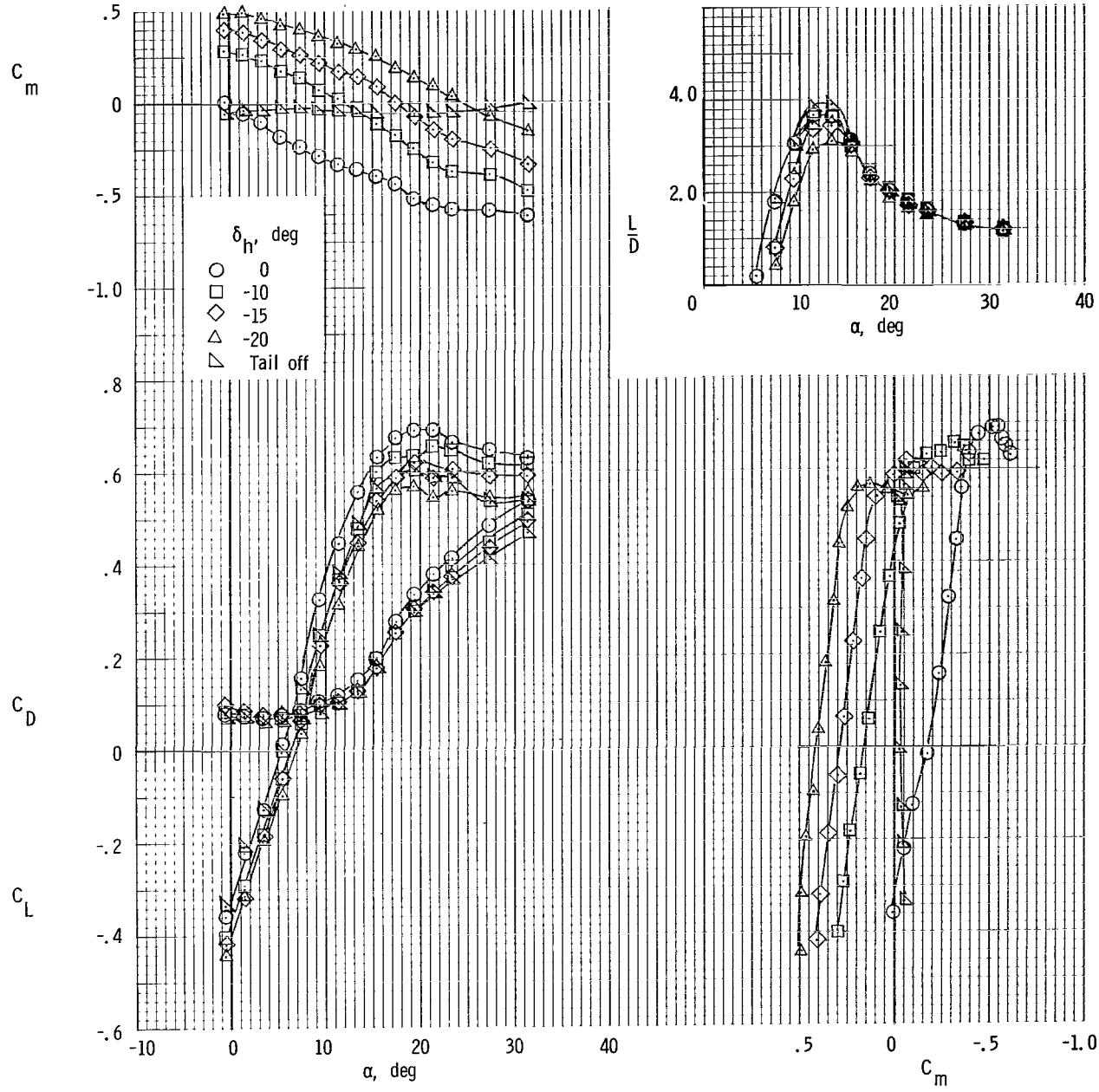

(b) Configuration II (small wing in high position).

Figure 10.- Continued.

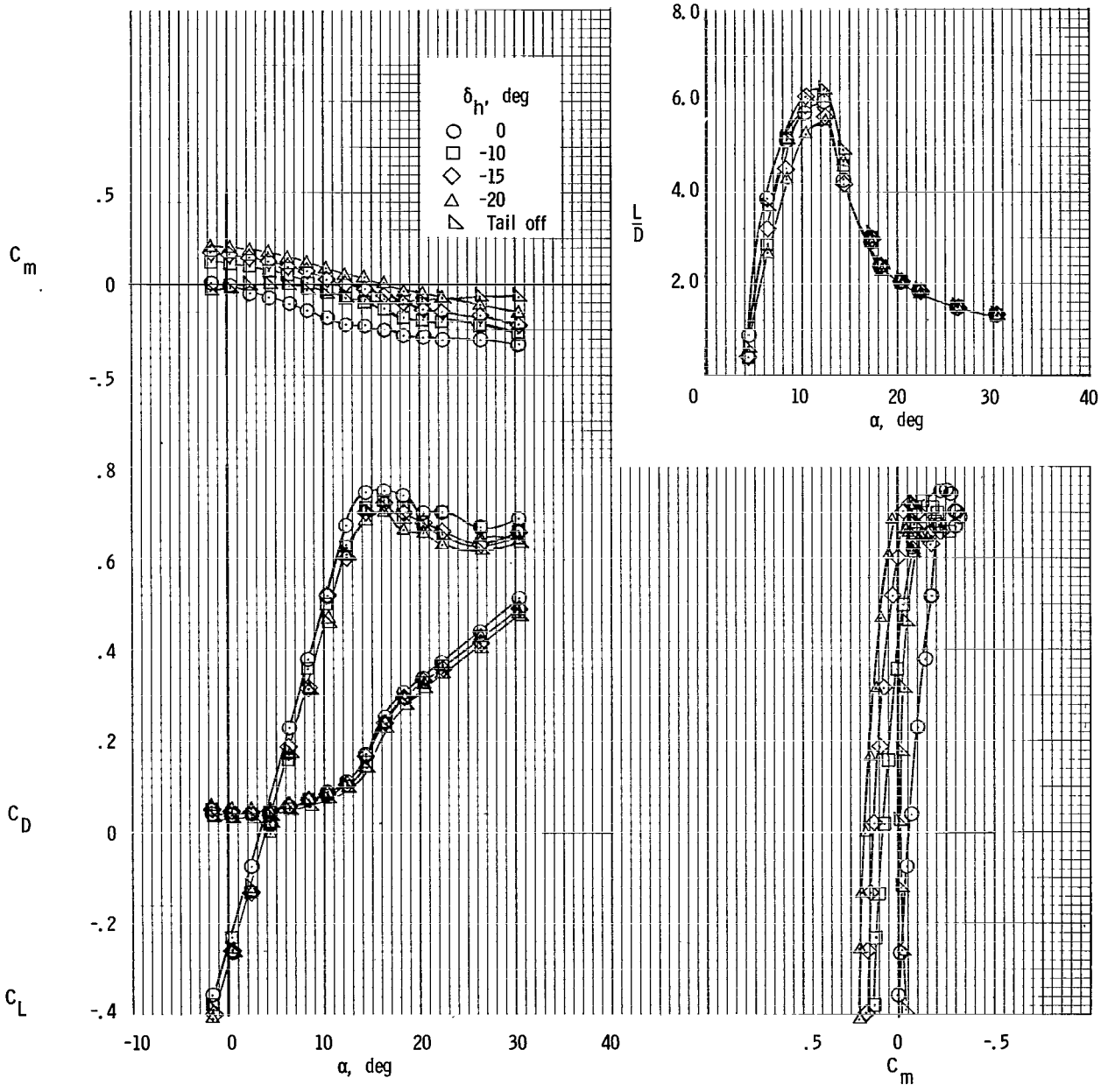

(c) Configuration III (large wing in high position).

Figure 10.- Concluded.

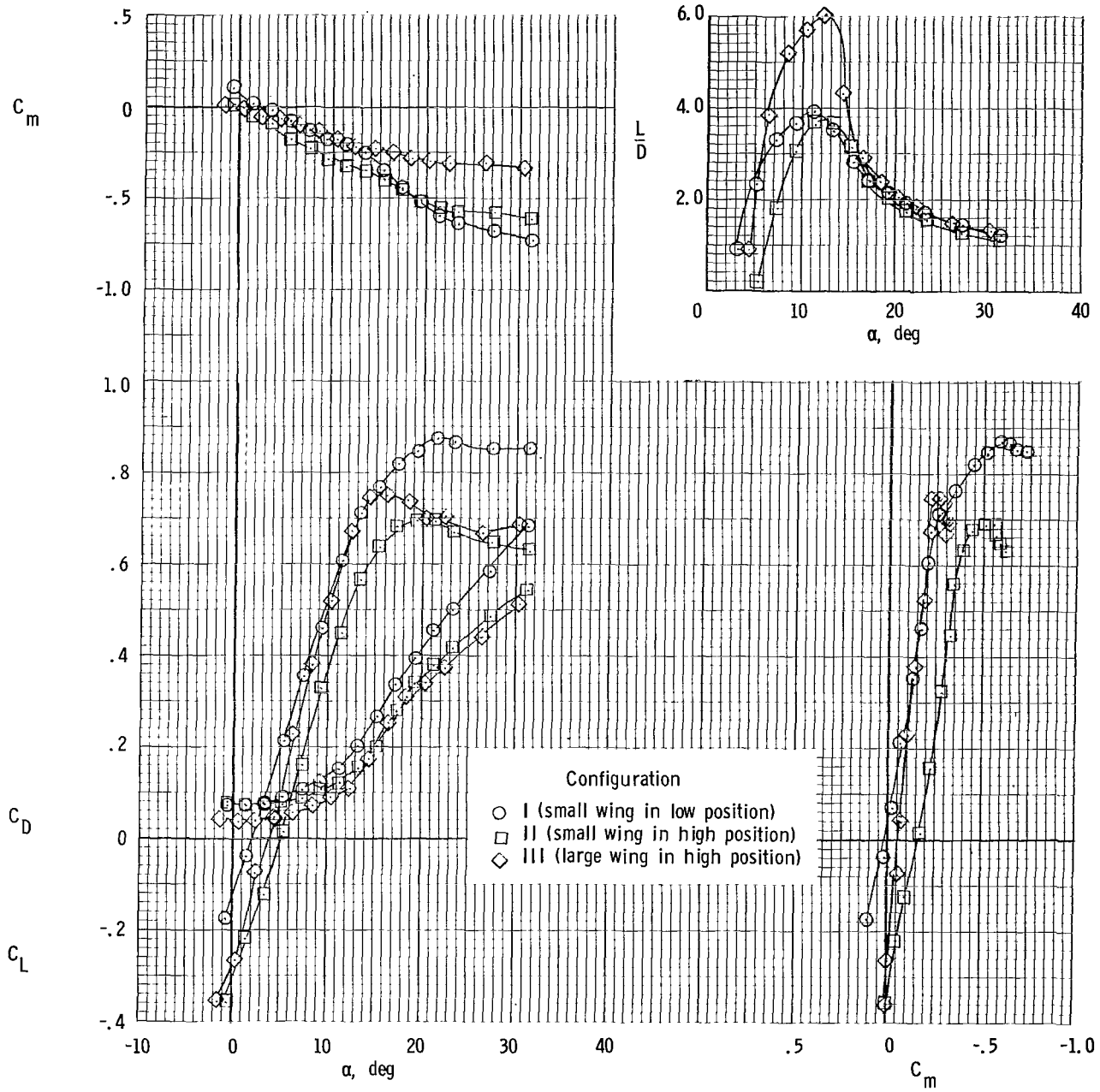

Figure 11.- Comparison of untrimmed longitudinal aerodynamic characteristics of complete-model configurations. Top vertical tail on; $\delta_h = 0^o$.

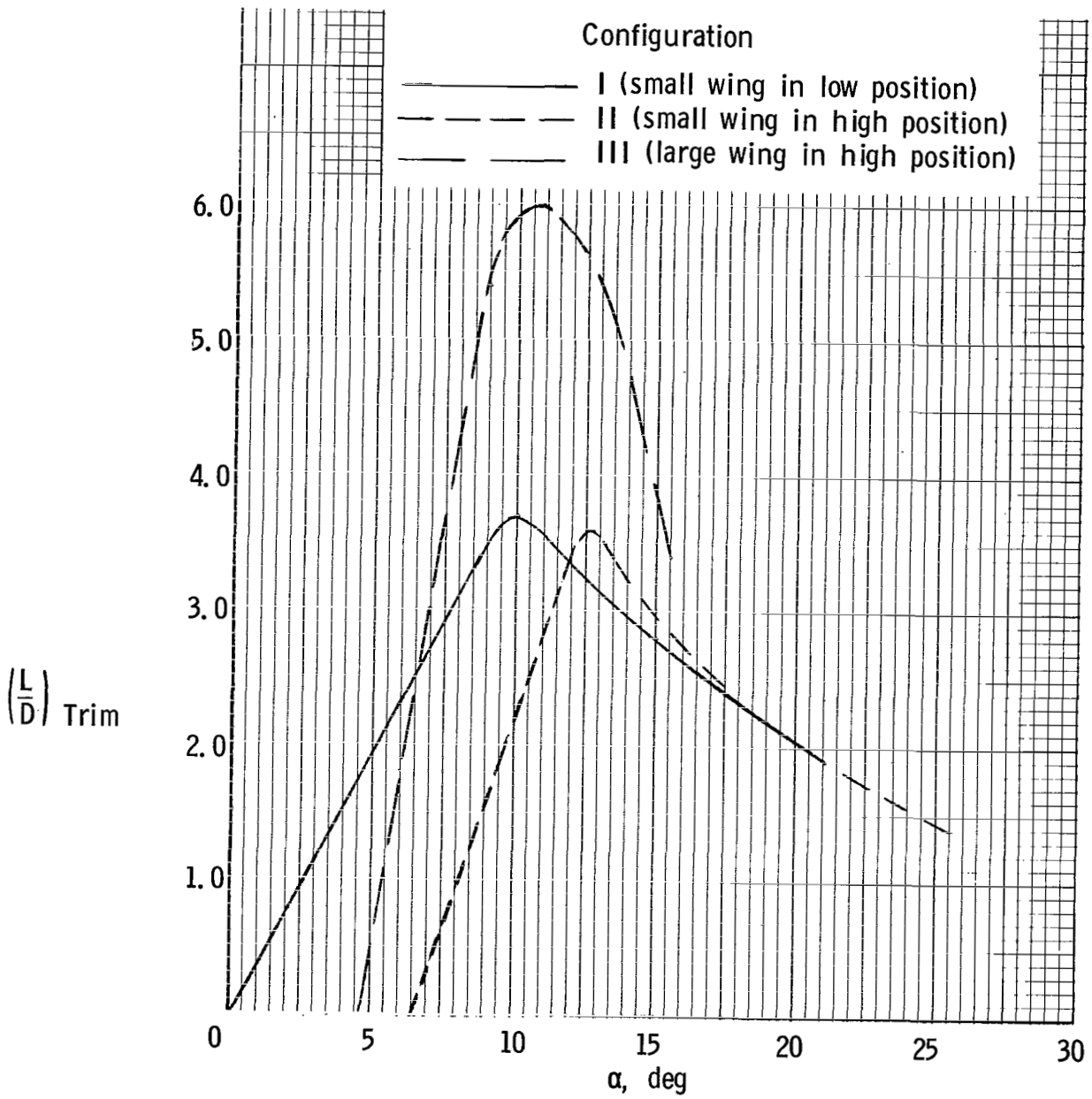

Figure 12.- Trimmed lift-drag ratio of complete-model configurations. Top vertical tail on.

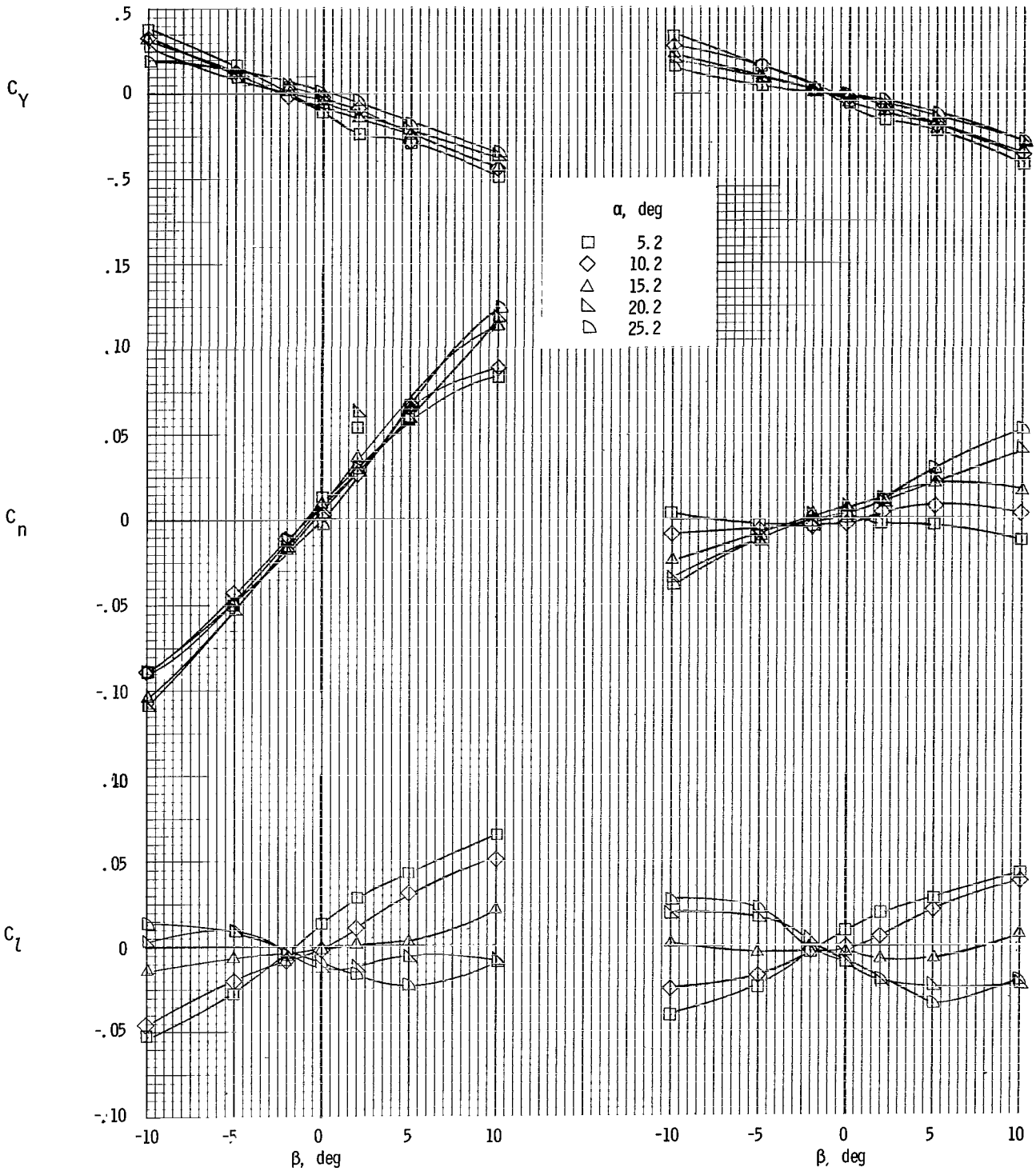

(a) Top and bottom vertical tails on.

(b) Top vertical tail on.

Figure 13.- Lateral characteristics of complete-model configuration I (small wing in low position). $\delta_h = -10^\circ$.

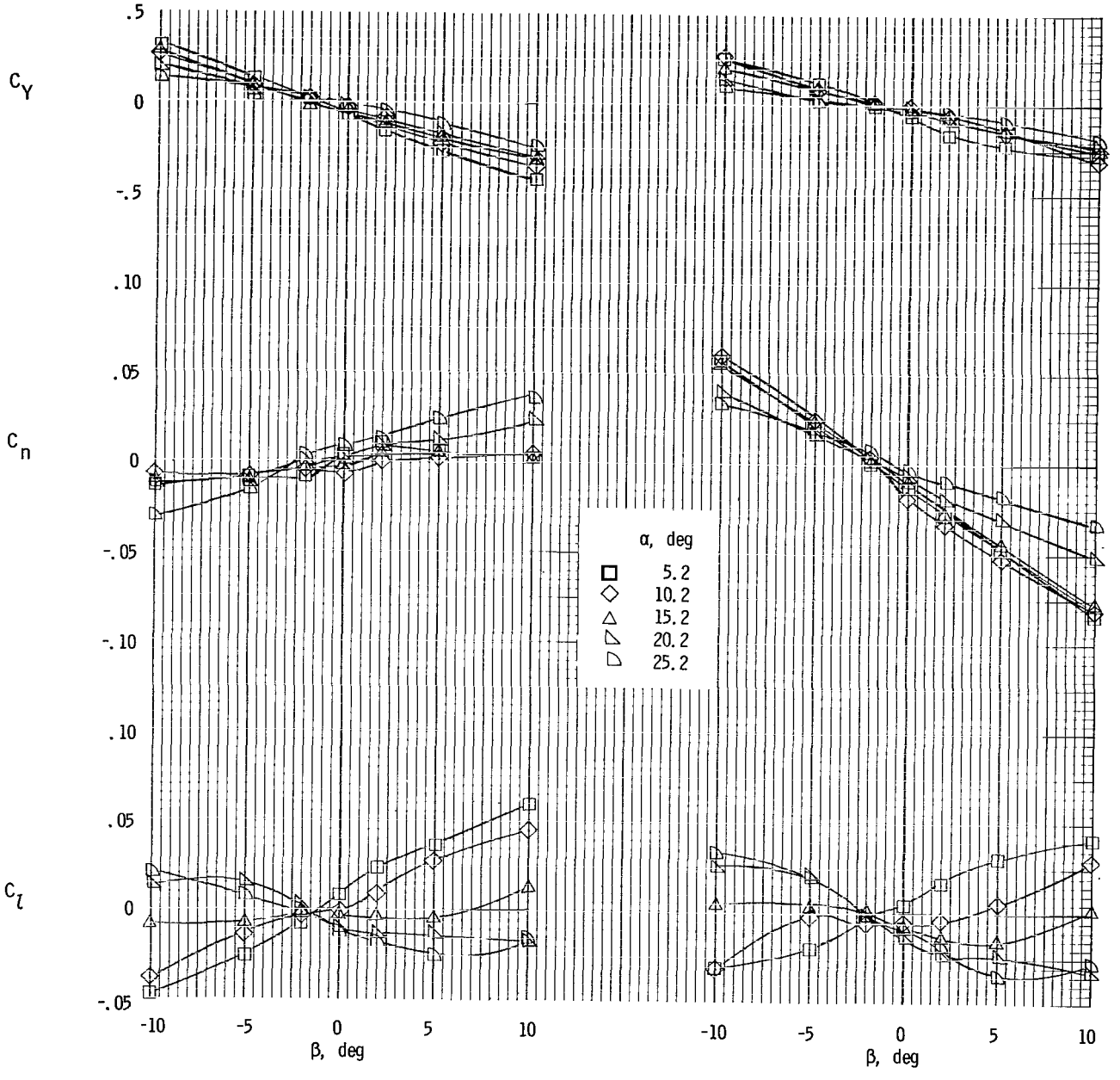

(c) Bottom vertical tail on.

(d) Vertical tails off.

Figure 13.- Concluded.

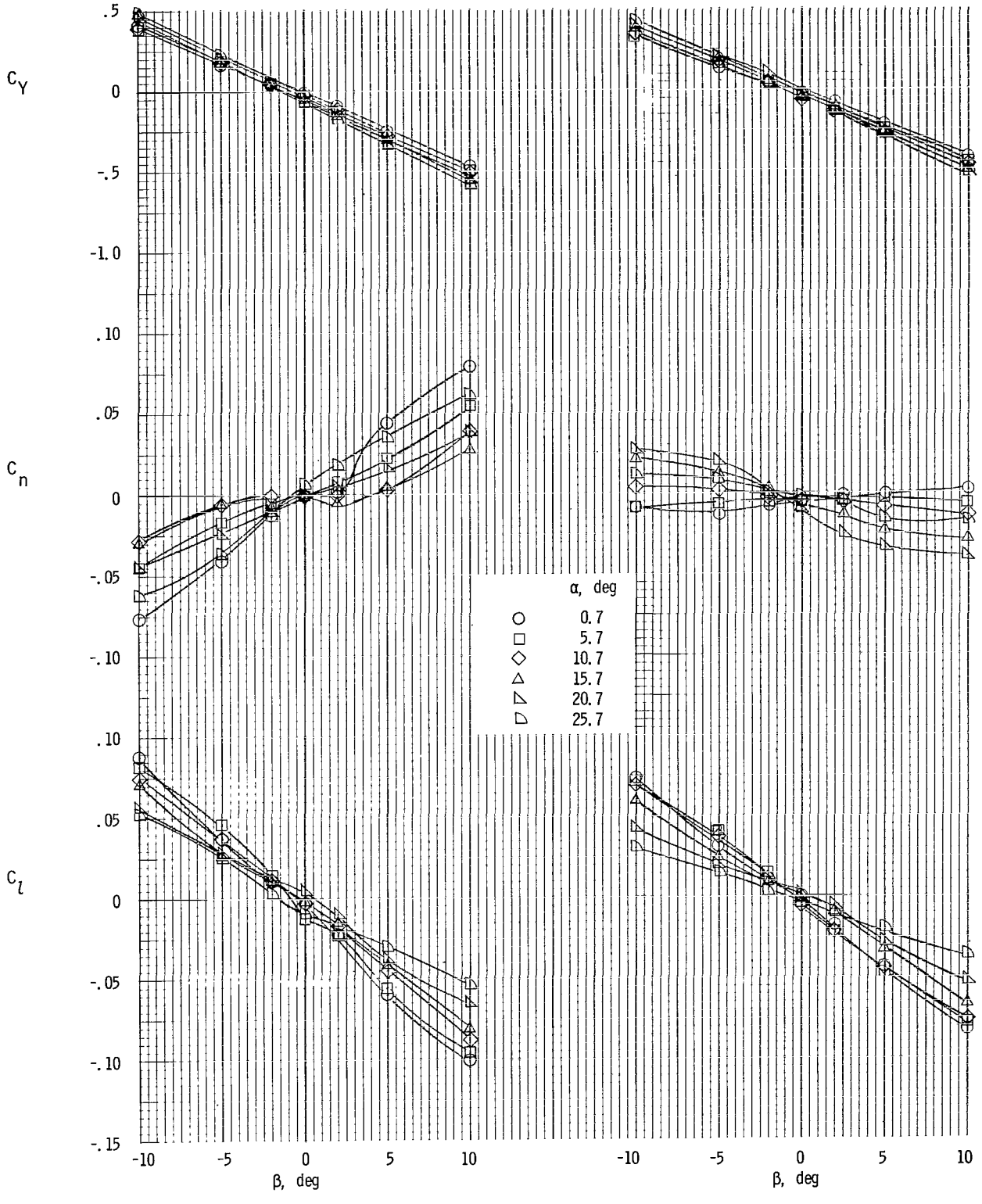

(a) Top and bottom vertical tails on.

(b) Top vertical tail on.

Figure 14.- Lateral characteristics of complete-model configuration II (small wing in high position). $\delta_h = -10^o$.

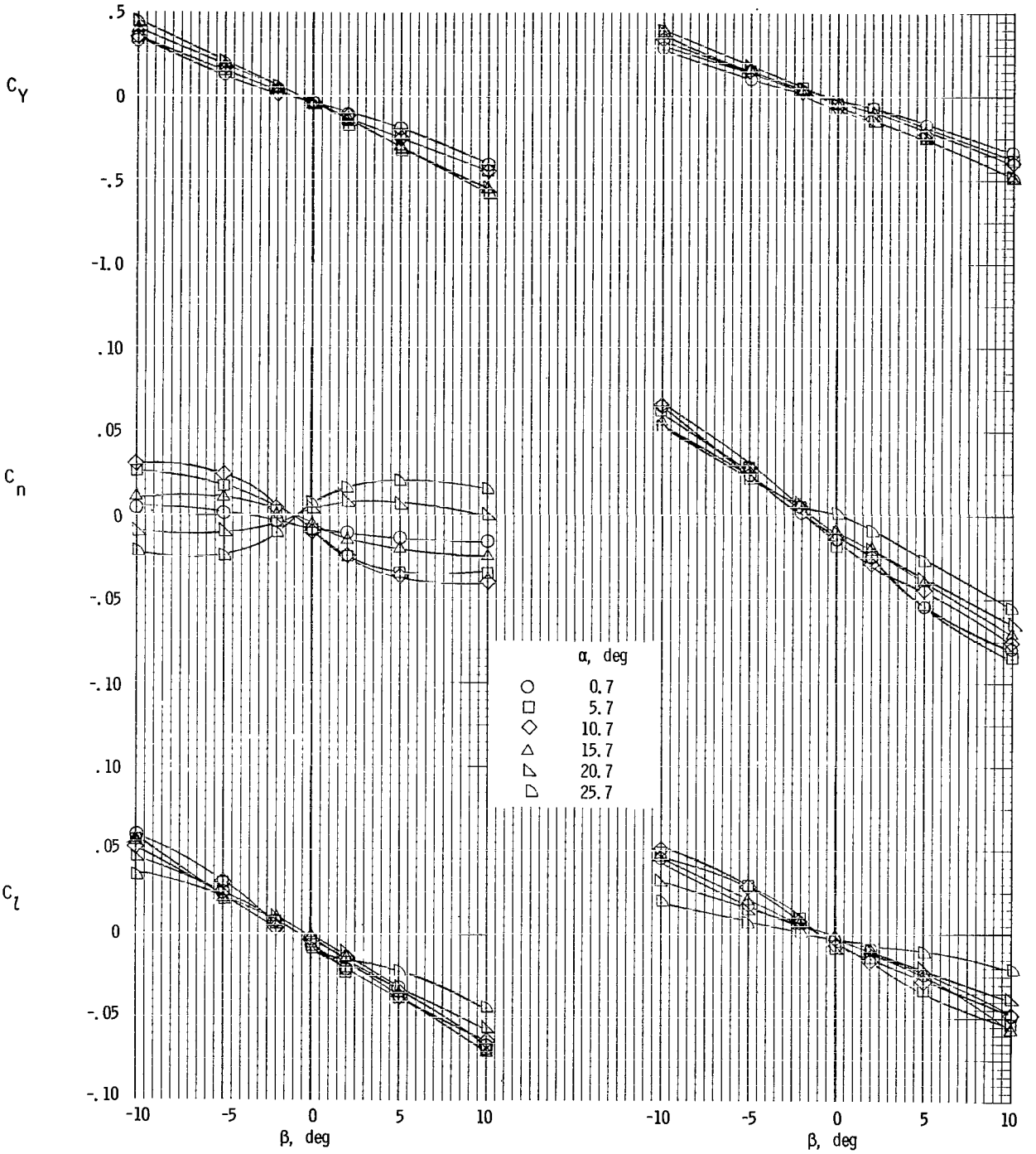

(c) Bottom vertical tail on.

(d) Vertical tails off.

Figure 14.- Concluded.

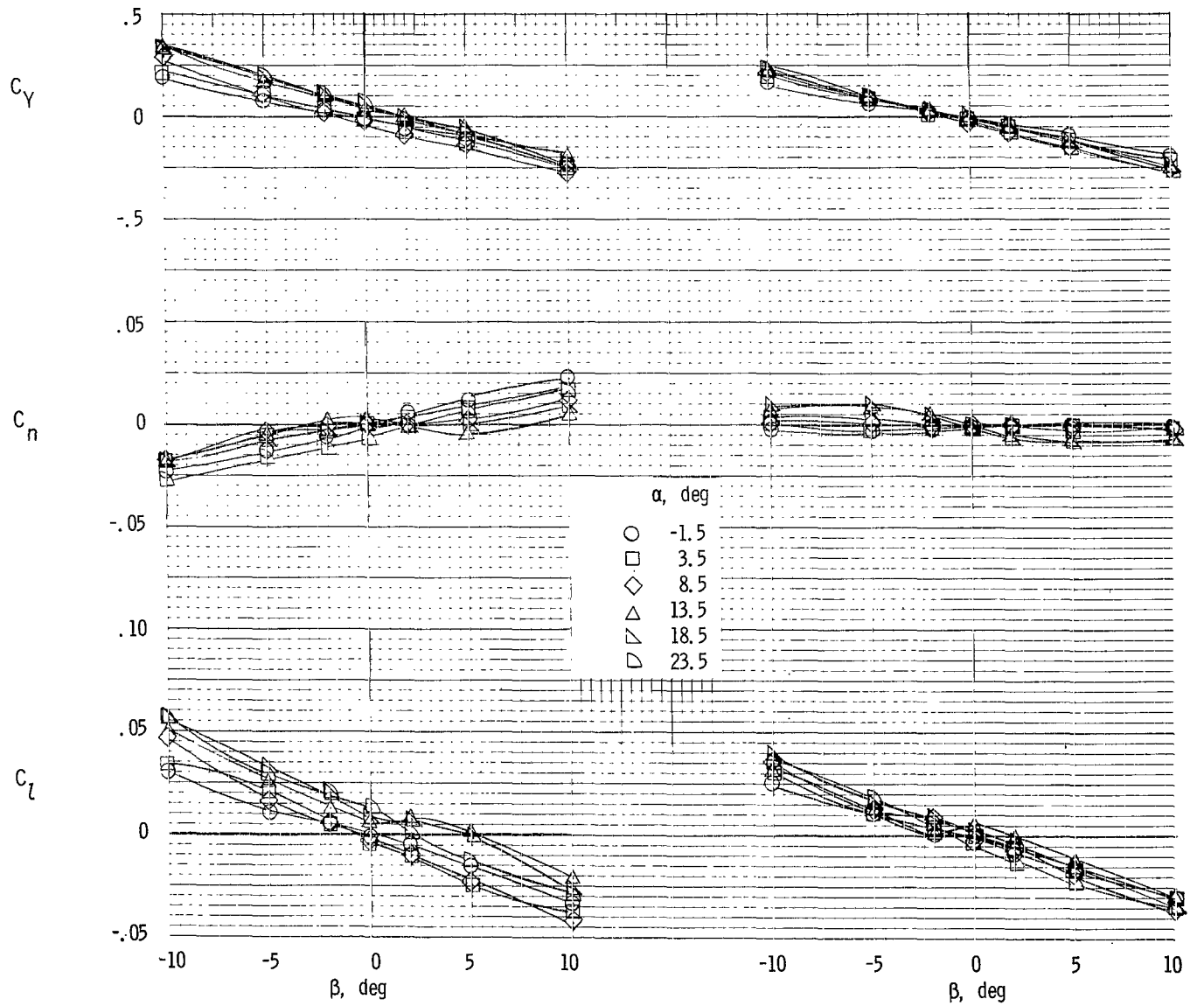

(a) Top and bottom vertical tails on.

(b) Top vertical tail on.

Figure 15.- Lateral characteristics of complete-model configuration III (large wing in high position). $\delta_h = -10^\circ$.

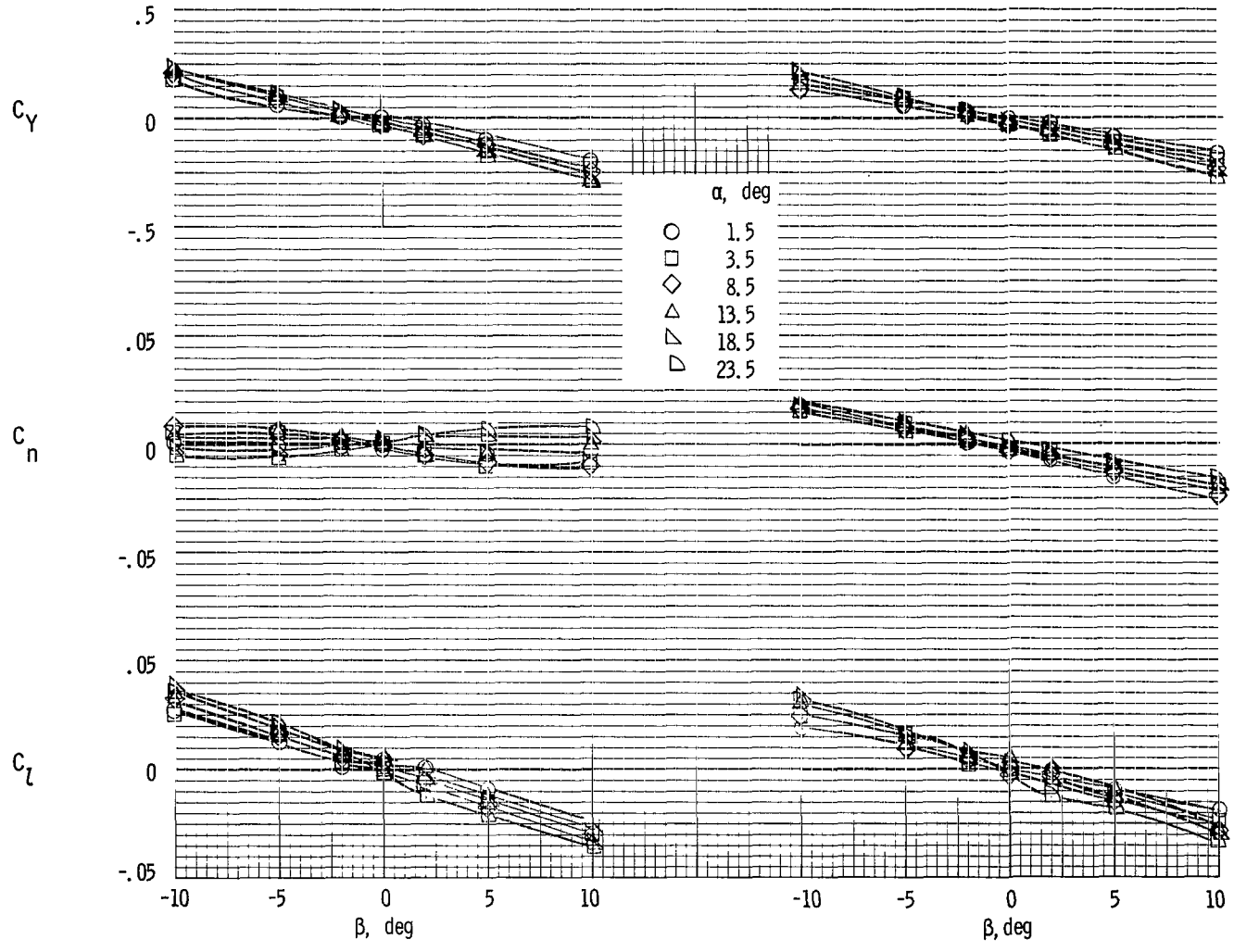

(c) Bottom vertical tail on.

(d) Vertical tails off.

Figure 15.- Concluded.

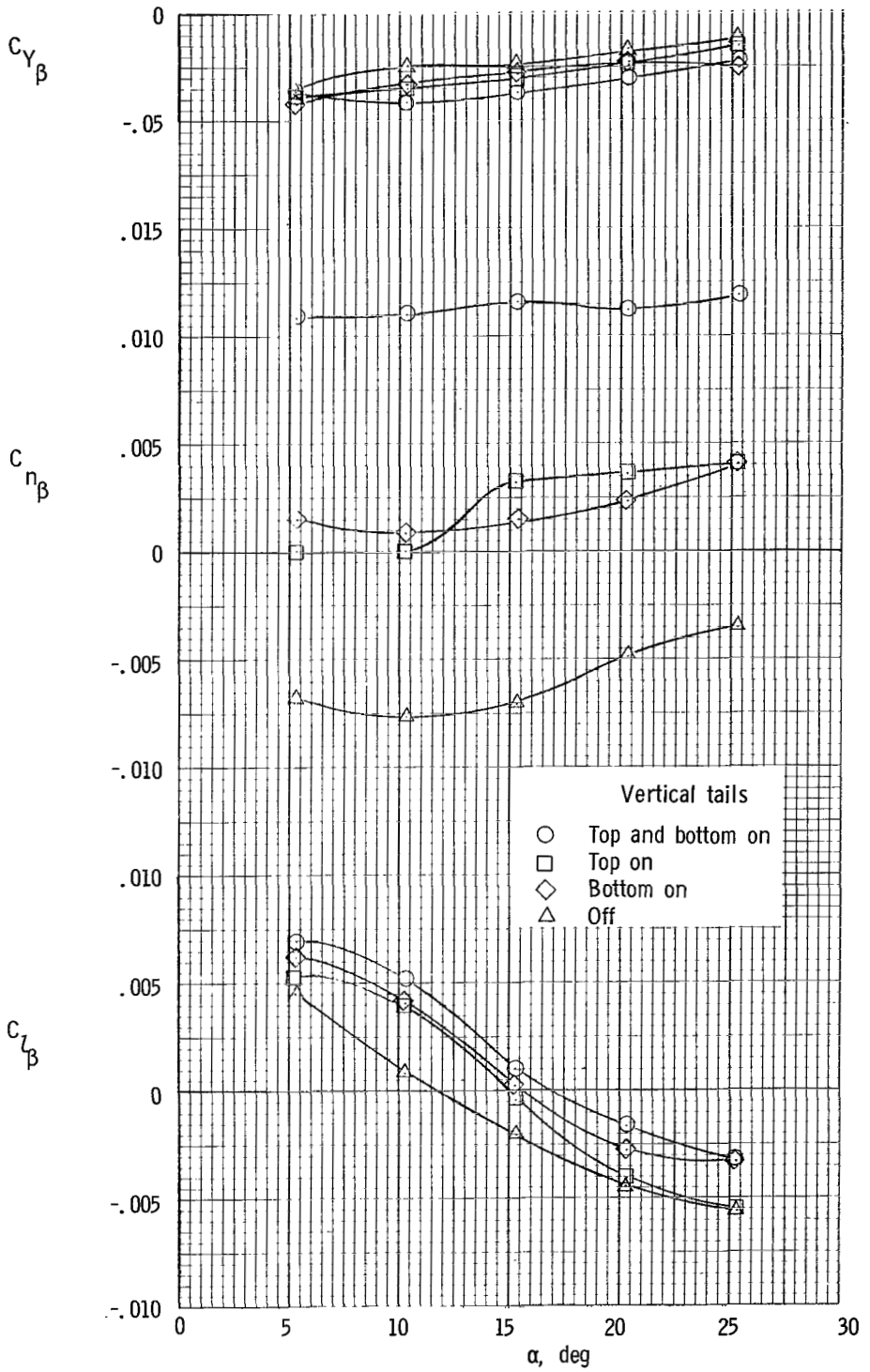

(a) Configuration I (small wing in low position).

Figure 16.- Effect of vertical-tail size and location on lateral stability characteristics of complete-model configurations. $\delta_h = -10^\circ$.

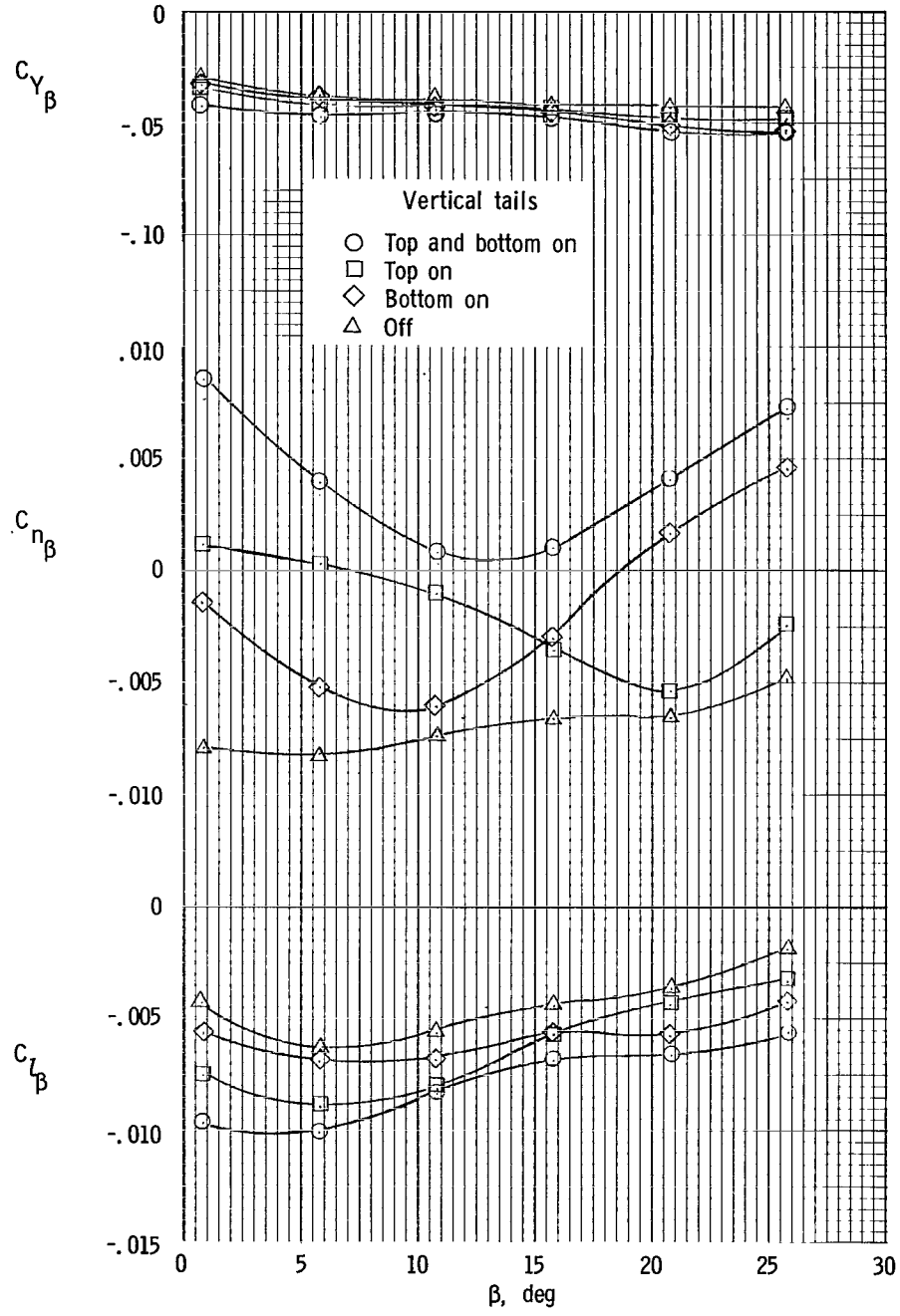

(b) Configuration II (small wing in high position).

Figure 16.- Continued.

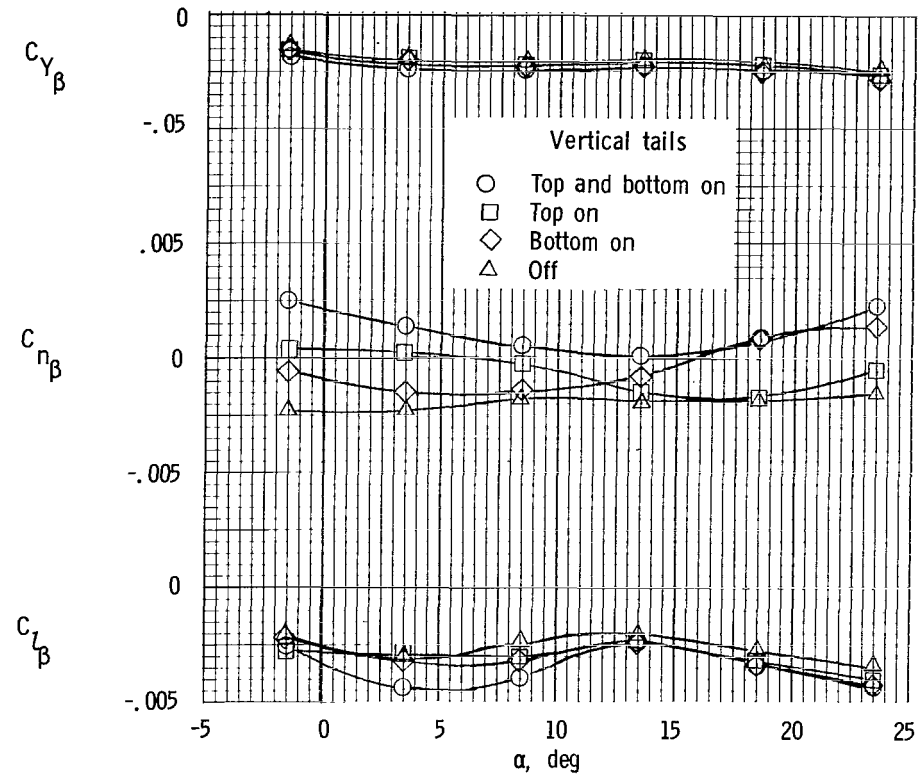

(c) Configuration III (large wing in high position).

Figure 16.- Concluded.

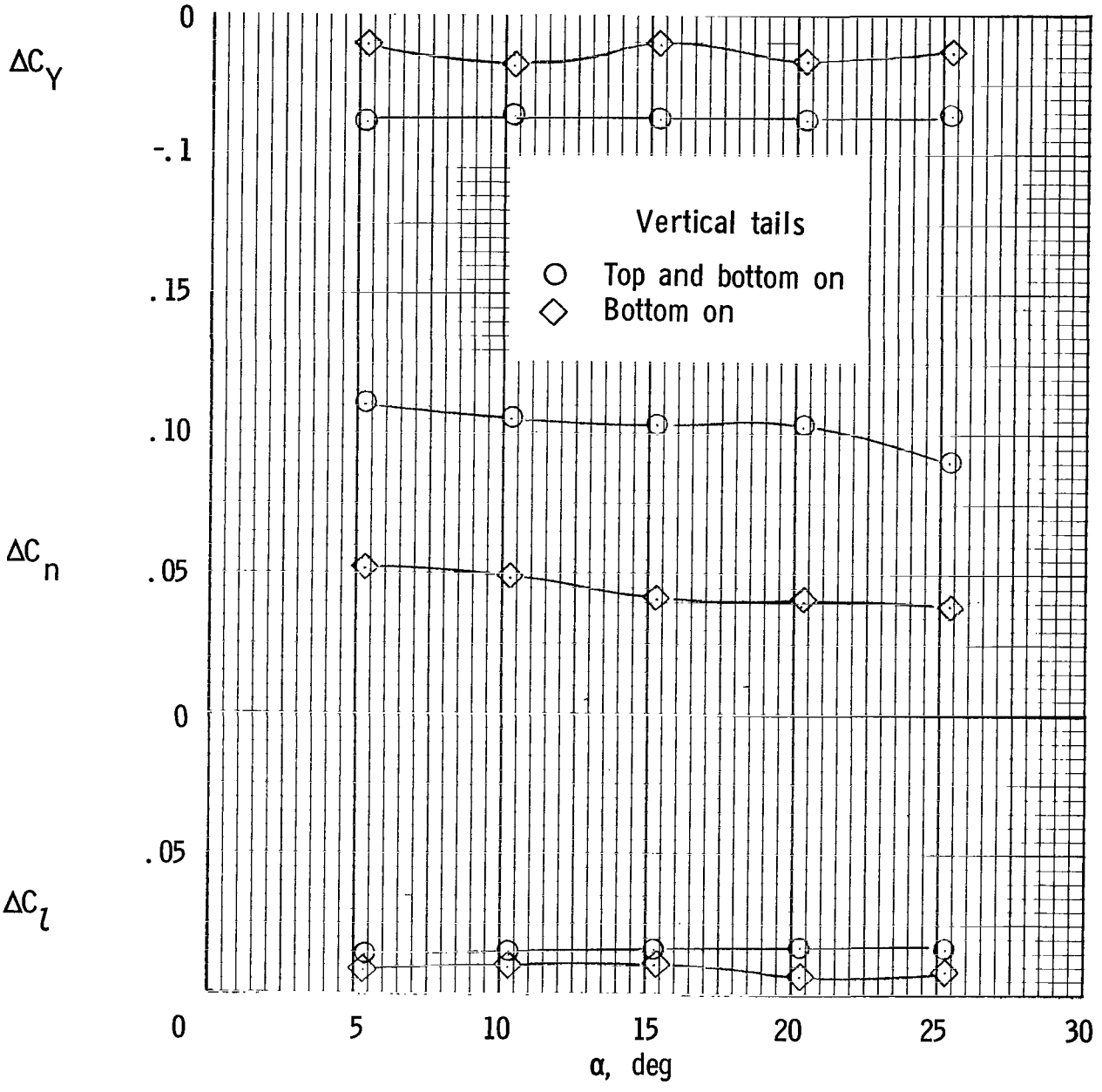

Figure 17.- Incremental lateral force and moments produced by all-movable vertical tail on complete-model configuration I (small wing in low position). $\delta_h = -10^o$.

"The aeronautical and space activities of the United States shall be conducted so as to contribute . . . to the expansion of human knowledge of phenomena in the atmosphere and space. The Administration shall provide for the widest practicable and appropriate dissemination of information concerning its activities and the results thereof."

—NATIONAL AERONAUTICS AND SPACE ACT OF 1958

NASA SCIENTIFIC AND TECHNICAL PUBLICATIONS

TECHNICAL REPORTS: Scientific and technical information considered important, complete, and a lasting contribution to existing knowledge.

TECHNICAL NOTES: Information less broad in scope but nevertheless of importance as a contribution to existing knowledge.

TECHNICAL MEMORANDUMS: Information receiving limited distribution because of preliminary data, security classification, or other reasons.

CONTRACTOR REPORTS: Scientific and technical information generated under a NASA contract or grant and considered an important contribution to existing knowledge.

TECHNICAL TRANSLATIONS: Information published in a foreign language considered to merit NASA distribution in English.

SPECIAL PUBLICATIONS: Information derived from or of value to NASA activities. Publications include conference proceedings, monographs, data compilations, handbooks, sourcebooks, and special bibliographies.

TECHNOLOGY UTILIZATION PUBLICATIONS: Information on technology used by NASA that may be of particular interest in commercial and other non-aerospace applications. Publications include Tech Briefs, Technology Utilization Reports and Notes, and Technology Surveys.

Details on the availability of these publications may be obtained from:

SCIENTIFIC AND TECHNICAL INFORMATION DIVISION

NATIONAL AERONAUTICS AND SPACE ADMINISTRATION

Washington, D.C. 20546